Chemical Engineering Journal 398 (2020) 125570

Contents lists available at ScienceDirect

Chemical Engineering Journal

journal homepage: www.elsevier.com/locate/cej

Comparison of *UV*-induced AOPs (*UV/Cl$_2$*, *UV/NH$_2$Cl*, *UV/ClO$_2$* and *UV/H$_2$O$_2$*) in the degradation of iopamidol: Kinetics, energy requirements and DBPs-related toxicity in sequential disinfection processes

Fu-Xiang Tian[a,*], Wen-Kai Ye[a], Bin Xu[b], Xiao-Jun Hu[a,*], Shi-Xu Ma[a], Fan Lai[a], Yu-Qiong Gao[c], Hai-Bo Xing[a], Wei-Hong Xia[a], Bo Wang[a]

[a] School of Chemical and Environmental Engineering, Shanghai Institute of Technology, Shanghai 201418, PR China
[b] State Key Laboratory of Pollution Control and Resources Reuse, Key Laboratory of Yangtze Water Environment, Ministry of Education, College of Environmental Science and Engineering, Tongji University, Shanghai 200092, PR China
[c] School of Environment and Architecture, University of Shanghai for Science and Technology, Shanghai 200093, PR China

HIGHLIGHTS

- Removal efficiency of iopamidol followed the order of *UV/Cl$_2$* > *UV/H$_2$O$_2$* > .
- *UV/NH$_2$Cl* > *UV/ClO$_2$* > *UV*.
- *EE/O* of iopamidol degradation followed the trend of *UV/ClO$_2$* > *UV* > *UV/NH$_2$Cl* > *UV/H$_2$O$_2$* > *UV/Cl$_2$*.
- The pH behaviors of *UV*-based AOPs upon iopamidol in 5–9 exhibited quite differently.
- *UV/Cl$_2$* and *UV/NH$_2$Cl* enhanced classical DBPs and I-THMs while *UV/ClO$_2$* and *UV/H$_2$O$_2$* exhibited elimination effect.
- The risk ranking of DBPs-related toxicity was *UV/NH$_2$Cl* > *UV/Cl$_2$* > *UV* > *UV/H$_2$O$_2$* > *UV/ClO$_2$*.

GRAPHICAL ABSTRACT

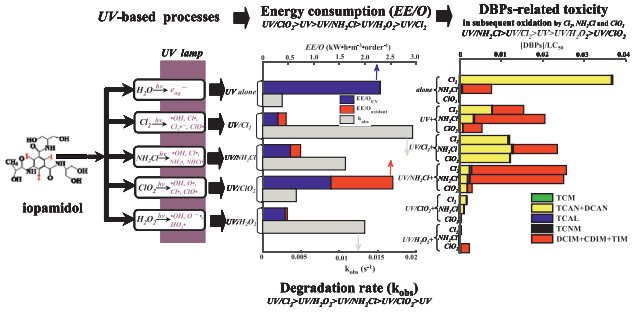

ARTICLE INFO

Keywords:
UV-based advanced oxidation processes (AOPs)
Degradation
Iopamidol
Electrical energy per order (*EE/O*)
Toxicity
Iodo-trihalomethanes (I-THMs)

ABSTRACT

The *UV*-induced advanced oxidation processes (AOPs, including *UV/Cl$_2$*, *UV/NH$_2$Cl*, *UV/ClO$_2$* and *UV/H$_2$O$_2$*) degradation kinetics and energy requirements of iopamidol as well as DBPs-related toxicity in sequential disinfection were compared in this study. The photodegradation of iopamidol in these processes can be well described by pseudo-first-order model and the removal efficiency ranked in descending order of *UV/Cl$_2$* > *UV/H$_2$O$_2$* > *UV/NH$_2$Cl* > *UV/ClO$_2$* > *UV*. The synergistic effects could be attributed to diverse radical species generated in each system. Influencing factors of oxidant dosage, *UV* intensity, solution pH and water matrixes (Cl^-, NH_4^+ and nature organic matter) were evaluated in detail. Higher oxidant dosages and greater *UV* intensities led to bigger pseudo-first-order rate constants (K_{obs}) in these processes, but the pH behaviors exhibited quite differently. The presence of Cl^-, NH_4^+ and nature organic matter posed different effects on the degradation rate. The parameter of electrical energy per order (*EE/O*) was adopted to evaluate the energy requirements of the tested systems and it followed the trend of *UV/ClO$_2$* > *UV* > *UV/NH$_2$Cl* > *UV/H$_2$O$_2$* > *UV/Cl$_2$*. Pretreatment of iopamidol by *UV/Cl$_2$* and *UV/NH$_2$Cl* clearly enhanced the production of

* Corresponding authors.
E-mail addresses: 13916841275@163.com (F.-X. Tian), hu-xj@mail.tsinghua.edu.cn (X.-J. Hu).

https://doi.org/10.1016/j.cej.2020.125570
Received 12 February 2020; Received in revised form 16 May 2020; Accepted 18 May 2020
Available online 30 May 2020

classical disinfection by-products (DBPs) and iodo-trihalomethanes (I-THMs) during subsequent oxidation while UV/ClO_2 and UV/H_2O_2 exhibited almost elimination effect. From the perspective of weighted water toxicity, the risk ranking was $UV/NH_2Cl > UV/Cl_2 > UV > UV/H_2O_2 > UV/ClO_2$. Among the discussed *UV*-driven AOPs, UV/Cl_2 was proved to be the most cost-effective one for iopamidol removal while UV/ClO_2 displayed overwhelming advantages in regulating the water toxicity associated with DBPs, especially I-THMs. The present results could provide some insights into the application of *UV*-activated AOPs technologies in tradeoffs between cost-effectiveness assessment and DBPs-related toxicity control of the disinfected waters containing iopamidol.

1. Introduction

At present, due to the worldwide outbreak of atypical pneumonia, caused by *COVID-19*, which is limitedly known to be sensitive to *UV* light and effectively killed by chlorine-based disinfectants, disinfection has never been valued so seriously by everybody [1,2]. Some investigators have proposed that *COVID-19* might have potential risks of water mediated transmission, which presents much stricter requirements and objectives for water disinfection [2]. However, more than 600 kinds of disinfection by-products (DBPs) have been accidentally found when chemical disinfectants are used to kill aquatic pathogens. The vast majority of DBPs have not been chemically or biologically characterized and only less than 100 kinds were resolved in quantitative occurrence or toxicity research centers [3]. DBPs are inevitably formed when commonly used disinfectants (Cl_2, O_3, ClO_2 or NH_2Cl, etc) react with naturally occurring organic matters in source waters during disinfection [3,4]. 11 types of DBPs, such as trihalomethanes (THMs) and haloacetic acids (HAAs), have been controlled in USA while 74 emerging DBPs are not regulated because of their medium occurrence levels or toxicological properties [3,4]. Besides, primary treatment with disinfectants is often followed by post disinfection to maintain disinfectants residues in water supply systems [5,6]. The occurrence of some emerging DBPs (for example, nitrogen-containing DBPs, iodo-DBPs (I-DBPs)) with highly enhanced toxicity might be unavoidable in this process [3,6].

The comparative toxicity order of different DBPs categories is iodination > bromination > chlorination [7]. This indicates that the more toxic I-DBPs are more worthy of studying on the health risk assessment in drinking water disinfection [3,8]. Among I-DBPs, which have attracted more and more attention nowadays, iodoacetic acid (IA) is an emerging drinking water pollutant with high toxicity. Studies have shown that IA is the most genotoxic DBPs in mammals [9,10]. Iodo-THMs (I-THMs) are the most detected I-DBPs species in drinking water. In addition to their far higher toxicity than conventional THMs, I-THMs could also cause other problems to potable water [11]. For example, iodoform has been considered as an important contributor to the incidents of bad tastes and odors, owing to its lowest organoleptic threshold concentration (0.03–1 μg L^{-1}) in all THMs [12]. In fact, it was estimated that up to 25% of bad taste and odor events in French drinking water were caused by iodoform [13,14]. Therefore, the regulation of I-DBPs is of great significance in lowering drinking water toxicity during disinfection. To achieve this goal, control measures on the transformation of iodine sources are extremely practical and operable.

Iopamidol is proved to be the most important organic iodine source of I-DBPs in drinking water [15,16]. The *UV* transformation characteristics of iopamidol to I-DBPs in subsequent oxidation processes have been reported in our previous work [15]. The degradation features and pathways of iopamidol in three *UV*-based advanced oxidation processes (AOPs, UV/Cl_2, $UV/S_2O_8^{2-}$ and UV/H_2O_2) were also studied [17,18]. Some investigators demonstrated that processes of O_3/H_2O_2 and UV/TiO_2 could also remove iodinated X-ray contrast media (ICM) including iopamidol [19,20]. Wang et al. studied the UV/Cl_2 degradation of iohexol (another important ICM) and I-THMs formation in the following chlorination [21]. Despite of so many reports on ICM degradation, most works concentrated on influence factors and destruction mechanisms in UV/Cl_2 and UV/H_2O_2, while UV/NH_2Cl and UV/ClO_2 have never been considered yet. Although the degradation of iopamidol by UV/Cl_2 and UV/H_2O_2 have been reported [17,18], the required electrical energy are still unknown and no effective measures haven been proposed to restrain its transformation to noxious I-DBPs. Thus, this study aimed to make overall comparisons of the *UV*-induced AOPs with respect to degradation characteristics, energy consumption and toxicity evaluation, especially the never touched processes of UV/NH_2Cl and UV/ClO_2.

Recently the *UV*-initiated AOPs, which combine *UV* irradiation with common oxidants (such as Cl_2, NH_2Cl, H_2O_2, $S_2O_8^{2-}$, HSO_5^-) or synthesized photocatalysts have attracted increasing interests in water treatment and environmental remediation fields [17,18,22–25]. Various highly reactive radicals can be formed in these integrated systems, which can apparently promote the degradation rate of organic contaminants compared with *UV* alone [17,18,24–26]. Research on iohexol indicated that UV/Cl_2 had more advantages than *UV* in controlling I-THMs [21]. Other studies on UV/Cl_2 also showed that higher Cl_2 concentrations could not only degrade ICM more effectively but also reduce the formation of I-THMs [27–29]. The *UV* photolysis of NH_2Cl can form $Cl\cdot$ and $NH_2\cdot$ while the former could directly or indirectly degrade many pollutants by forming $\cdot OH$ [30–32]. Although UV/NH_2Cl might inhibit the degradation of organic compounds and promote the DBPs formation in actual waters, the removal effect was fairly satisfactory [23,33]. H_2O_2 can also be *UV* photolyzed directly to form $\cdot OH$ and the highly reactive $\cdot OH$ is considered to play the most important role as it could attack organic compounds by inducing a series of oxidation reactions [34–38]. However, the evolution of iopamidol in these *UV*-based AOPs and their effects on the formation of I-DBPs in subsequent oxidation are still not clear.

The four *UV*-based systems related here (UV/Cl_2, UV/NH_2Cl, UV/ClO_2 and UV/H_2O_2) are quite different in oxidation ability, application convenience as well as performance-to-price ratio. Generally speaking, the free radicals involved in these processes mainly include reactive oxygen species (ROS), reactive chlorine species (RCS) and nitrogen-containing radicals. There are great differences in the reaction selectivity between these two kinds of radicals towards organic compounds, which make the oxidized intermediates of the same target compound quite differently and then have a significant impact on the DBPs-related toxicity of waters in subsequent oxidation. Few studies have specifically concerned the resulted water toxicity associated with DBPs derived from these intermediates. So it is of important guiding significance in practical applications for these processes to study the degradation efficiency and energy requirements of pollutants in these AOPs, as well as their effects on water toxicity. Considering the high *UV* photosensitivity of ICM [15,17,18], there is clearly much work to be done to examine the removal characteristics of iopamidol by different *UV*-based AOPs and their influence on the transformation of nontoxic iodinated medicine to toxic I-DBPs.

The objectives of present work are (1) to compare the removal efficiency and degradation kinetics of iopamidol by four *UV*-induced AOPs (UV/Cl_2, UV/NH_2Cl, UV/ClO_2 and UV/H_2O_2) in terms of oxidant dosage, *UV* intensity, solution pH and water matrixes (Cl^-, NH_4^+ and nature organic matter (NOM)); (2) to evaluate the energy consumption of these systems using electrical energy per order (*EE/O*) parameter; (3) to estimate DBPs (including classical DBPs and I-THMs) formation and

the related toxicity during subsequent oxidation. The current research could provide some insights into the application of *UV*-mediated AOPs technologies in tradeoffs between cost-effectiveness assessment and toxicity control associated with DBPs, especially I-THMs, of the disinfected waters containing iopamidol.

2. Experimental materials and methods

2.1. Chemicals and reagents

All the reagents used in this research were at least analytical purity except as noted. Iopamidol (99.6%) was obtained from U.S. Pharmacopeia. The calibration standards for 18 kinds classical DBPs (including dibromochloromethane (DBCM), bromodichloromethane (BDCM), chloroform (TCM), bromoform (BF), dichloropropanone (DCP), trichloroacetone (TCP), bromochloroacetonitrile (BCAN), dichloroacetonitrile (DCAN), trichloroacetonitrile (TCAN), dibromoacetonitrile (DBAN), trichloroacetaldehyde (TCAL), trichloronitromethane (TCNM), dibromoethane (DBE), trichloroethane (TCE), trichloroethylene, tetrachloromethane, tetrachloroethylene and dibromochloropropane), KH_2PO_4 (≥99.0%), iodoform (TIM, CHI_3, 99%), Na_2CO_3 (≥99.0%), *NaOH* (≥98%), NH_4Cl (≥98%), $NaHCO_3$ (≥99.0%) and *NaOCl* (available Cl_2 as 4.00–4.99%) were all acquired from Sigma-Aldrich (St. Louis, MO, USA). Acetonitrile and methyl *tert*-butyl ether (MtBE) were obtained from J.T. Baker (USA). The standards of I-THMs including bromodiiodomethane (BDIM, $CHBrI_2$, 90–95%), dibromoiodomethane (DBIM, $CHBr_2I$, 90–95%), dichloroiodomethane (DCIM, $CHCl_2I$, ≥95%), chlorodiiodomethane (CDIM, $CHClI_2$, 90–95%) and bro-mochloroiodomethane (BCIM, *CHBrClI*, ≥95%) were all bought from CanSyn Chemical Corp. (Canada). H_2O_2, $Na_2S_2O_3$, $K_2TiO(C_2O_4)_2$, *NaCl*, benzoic acid (BA), *tert*-butanol (TBA), H_2SO_4 and other chemicals of analytical purity were obtained from Sinopharm Chemical Reagent Co., Ltd. (Shanghai, China). Ultra-pure water generated from a Milli-Q water purification system (Millipore, USA) were used to prepare all the solutions here.

NH_4Cl and *NaOCl* (molar ratio of Cl_2/N = 0.8:1) at pH 8.5 were newly mixed to prepare NH_2Cl solution [39]. Stock solution of ClO_2 was generated freshly to ensure the purity using the modified method detailed previously [40]. The water matrix of real water was used as NOM sources in this study. The real water samples were acquired from the river running through our university and purified by 0.45 μm membranes (Millipore Corp., Billerica) before used. The main water characteristics of real waters were given in Table S10.

2.2. Procedures of experiments

The experiments on the degradation of iopamidol by different *UV*-based processes (*UV* alone, UV/Cl_2, UV/NH_2Cl, UV/ClO_2 and UV/H_2O_2) were carried out in a photoreactor equipped with four Hg *UV* lamps of low pressure (TUV11WT54P-SE, Philips, Netherlands) described elsewhere in our former reports [15,41].

Iopamidol solution with original concentration of 10 μM was spiked with certain dosages of different oxidants (Cl_2, NH_2Cl, ClO_2 and H_2O_2) and dosed with 10 mM buffer in advance (phosphate for pH 5–8 and carbonate for pH 9). Then it was adjusted to the predefined pH. The *UV* intensity was altered by simultaneously unlocking different numbers of lamps after being preheated for 30 min. Then a 200-mL solution with 10 μM iopamidol and certain oxidant concentration was subjected to *UV* light at 25 °C. At the proper time intervals, 1 mL sloution was instantly transferred from the reactor to a high performance liquid chromatography (HPLC) vial containing configured volume of $Na_2S_2O_3$ to quench the reaction and then analyzed by HPLC immediately. For ease of comparison, studies on the degradation of iopamidol within 300 s by the discussed *UV*-based processes were investigated uniformly.

In DBPs (including classical DBPs and I-THMs) formation experiments, the iopamidol solution spiked with certain dose oxidant (Cl_2, NH_2Cl, ClO_2 and H_2O_2) was exposed to the same *UV* fluence to realize a complete transformation of iopamidol. Then certain volume of $Na_2S_2O_3$ was added, which was calculated based on the residual concentration of oxidant measured after the photochemical reaction. Afterward, triplicate samples in 40-mL glass under headspace-free conditions were then placed into an incubator, which was kept in dark for 25 °C inside. After being incubated for 7 days, the samples were quenched with NH_4Cl (20% in excess) and then were extracted by MtBE for classical DBPs and I-THMs analysis, respectively.

2.3. Analytical techniques

Analytical informations of the chemicals (including iopamidol, classical DBPs and I-THMs) detected in this study were presented in Table S1.

The analysis of iopamidol was achieved by HPLC (Shimadzu LC-20A) with a XTerra® MS C_{18} column (4.6 × 250 mm i.d., 5 μm film thickness, Waters, USA) and an *UV* detector at wavelength of 242 nm [15]. Volume ratio of 1:9 between acetonitrile and water and flow rate of 0.80 mL min^{-1} was used. The analytic limitation was 10.0 μg L^{-1} and 10 μL of the injection volume was intercalated for detection.

The analytical methods of classical DBPs and I-THMs were modified based on USEPA Method 551.1 [15,42]. The treated samples were extracted by MtBE and then analyzed by a gas chromatograph (GC-2010, Shimadzu, Japan) fixed with an electron capture detector and a HP-5 capillary column (30 m × 0.25 mm i.d., 0.25 μm film thickness, J&W, USA). The oxidized samples were adjusted to pH 5–6 before detecting total organic carbon (TOC) as well as total nitrogen (TN) and then analyzed by TOC-L (Shimadzu, Japan) with ASI-L auto-sampler. The detection limit of TOC was 0.1 mg L^{-1}. UV_{254} was detected by an *UV*–Vis spectrophotometer (SQ-4802 UNICO, Shanghai) via a 1-cm quartz cell·H_2O_2 was quantified by the titanium oxalate method spectrophotometrically [43]. The concentrations of Cl_2 and NH_2Cl were both detected by the N, N-diethyl-p-phenylenediamine (DPD) method [44]. ClO_2 was calibrated by a DR/890 colorimeter (Hach, USA) [40].

The analysis of iopamidol intermediates by different *UV*-based AOPs was acquired by Fourier transform-ion cyclotron resonance-mass spectrometry (FT-ICR-MS). MS was performed with a Bruker 7.0 T solariX FT-ICR-MS (Bruker Daltonics, Bremen, Germany) equipped with an ESI source. The following MS conditions were applied: the sample solution flow rate was 120 μL h^{-1}, the drying temperature was set at 200 °C, the drying gas flow rate was 4.0 L min^{-1}, the nebulizer was 1.0 bar, the capillary voltage was 4500 V and the mass range was recorded from *m/z* 100 to 1000 Da in a positive-ion mode.

Standard buffer solutions (pH = 4.01, 7.00, 9.21) were frequently applied to calibrate the pH meter for pH measurement (FE20-FiveEasy, Mettler Toledo, Switzerland). *UV*-C luxometer (Photoelectric Instrument Factory of Beijing Normal University, Beijing, China) placed into a quartz sleeve inside the reactor was used to measure the exposed light intensity, which were altered by turning on 1, 2, 3 and 4 lamps (measured to be 2.43, 4.94, 7.34 and 9.76 mW cm^{-2}, respectively).

3. Results and discussions

3.1. Degradation efficiency of iopamidol by different UV-induced processes

The degradation of pollutants by UV/Cl_2 [17,18,26,27,45,46], UV/NH_2Cl [30,47–49], UV/ClO_2 [50–52] and UV/H_2O_2 [53–56] processes are developed and the kinetics could be depicted by pseudo-first-order model with regard to the compound concentration, as explicated in Eq. (1).

$$-\frac{dC}{dt} = k_{obs}t \quad (1)$$

The following Eq. (2) can be acquired by integrating Eq. (1):

$$\ln \frac{C_0}{C_t} = k_{obs} t = (k_{radicals} + k_{UV} + k_{oxidant})t \quad (2)$$

where k_{obs} represents rate constant of the pseudo-first-order reaction, t is the corresponding reaction time, C_0 and C_t stand for the initial and instant concentrations of iopamidol. The total decomposition of iopamidol can be attributed to the degradation contribution of reactive radicals ($k_{radicals}$), *UV* irradiation (*EE*/*O*) and the oxidant itself ($k_{radicals}$), respectively, viz.,

$$k_{obs} = k_{radicals} + k_{UV} + k_{oxidant} \quad (3)$$

[17,30,47,51,56]. Our previous studies have reported the oxidation rate constants of iopamidol by Cl_2 and NH_2Cl, which revealed the negligible degradation of the target compound after 300 s reaction (the same data shown in Fig. S1) [57]. It was also found that both H_2O_2 and ClO_2 can not oxidize iopamidol evidently (data also shown in Fig. S1) within 300 s [17,18]. Hence the values of $k_{oxidant}$ in the respective system can be neglected. Therefore, the k_{obs} can be simplified as:

$$k_{obs} = k_{radicals} + k_{UV} \quad (4)$$

The *UV* degradation of iopamidol has also been proposed to follow pseudo-first order kinetics [15]. To compare these *UV*-induced AOPs, the degradation of iopamidol was thus evaluated firstly, as depicted in Fig. 1.

As presented in Fig. 1, linear regression curves of different *UV*-based processes were determined ($R^2 > 0.99$) and the respective slopes (representing k_{obs}, listed in Fig. S2) were then obtained. Comparatively, iopamidol underwent mildly direct photolysis by *UV* alone (k_{obs} calculated to be 0.002551 s^{-1}). The combination of *UV* radiation with oxidants (Cl_2, NH_2Cl, ClO_2 and H_2O_2) can markedly promote the degradation rate of iopamidol. The negligible direct oxidation of Cl_2, NH_2Cl, ClO_2 and H_2O_2 towards iopamidol (Fig. S1) enabled the comparison among *UV*-based systems as depicted in Fig. S2. Obviously, among the five processes, k_{obs} followed the order of *UV*/Cl_2 (0.01954 s^{-1}) > *UV*/H_2O_2 (0.01330 s^{-1}) > *UV*/NH_2Cl (0.01079 s^{-1}) > *UV*/ClO_2 (0.004388 s^{-1}) > *UV*. The synergistic effects of these processes could be explained by various reactive radicals generated by irradiation of oxidants, as summarized in Tables S2–S5. The diverse radical species (for example, ROS, RCS and nitrogen-containing radicals) within each system can attack different functional groups in iopamidol, which resulted in the distinct degradation rates.

UV/Cl_2 exhibited the highest oxidation performance towards iopamidol, due to the comprehensive action of *UV* photons, the primary radicals (·*OH* and *Cl*·) as well as the secondary radicals (Cl_2·$^-$ and *ClO*·), especially the aftermost [17,18]. It is reported that the *UV* photolysis rate of chlorines is much higher than that of H_2O_2 [18,29,46,58]. The highly selective RCS were supposed to be the major contributors while *UV* photolysis constituted only 13.055% during the *UV*/Cl_2 degradation of iopamidol. The quenching experiments applying BA and TBA were performed (Text S1 and Figs. S3(a), (b)), which indicated that the major contributing radicals were Cl_2·$^-$ and *ClO*·. The results were consistent with the reported studies [17,18].

The major contributing radical in *UV*/H_2O_2 was believed to be ·*OH* [18,35,56] and this can also be demonstrated by the quenching experiments of TBA (Text S1 and Fig. S3(f)). It was calculated that ·*OH* contributed 80.82% of the total iopamidol degradation (Fig. 1), the reaction rate constant of which reported to be $(3.42 \pm 0.28) \times 10^9$ M^{-1} s^{-1} [59]. NH_2Cl, which slowly releases *HClO*, would decompose by *UV* to produce *Cl*· and NH_2· (reaction (1) in Table S3) [47], and *Cl*· will then continue to produce ·*OH* (reactions (2)–(4) in Table S3) [30]. Although the direct oxidant was NH_2Cl, it was the indirect oxidants of free chlorine (*HOCl* and OCl^-) that motivated the following oxidation of iopamidol. *Cl*· and ·*OH* were suggested to be the major contributing radicals in *UV*/NH_2Cl responsible for the degradation of iopamidol [48,49], with *UV* photolysis accounted for only 23.65% of the total degradation. This could be confirmed by the radical quenching experiments by TBA and BA (Text S1 and Figs. S3(c)–(d)). Meanwhile, nitrogen-containing radicals (NH_2· and *NHCl*·) made minor contributions. Though *UV*/Cl_2 and *UV*/NH_2Cl both yield ·*OH* and RCS, the major contributing radicals differed and *UV*/Cl_2 turned out to be much effective.

Although the degradation rate of iopamidol in *UV*/ClO_2 behaved the lowest, the synergistic effect of *UV* irradiation coupled with ClO_2 was remarkable compared with either single treatment. *UV* contributed up to 58.14% of the total iopamidol degradation, which suggested the secondary role of radicals in *UV*/ClO_2. It is reflected from another angle that the yields of radicals (including ·*OH*, ·*O*, *Cl*· and *ClO*· in Table S4) were too limited to present a high k_{obs} value. Scavenger study using TBA stated that ·*O* was the major contributing radical while other radicals made minor contributions (Text S1 and Fig. S3(e)). There's hardly any study inquiring into the radical speciations of *UV*/ClO_2 and more work should be done to distinct the respective contributions of radicals involved.

Simply from the degradation efficiency point of view, *UV*/Cl_2 technology was the first choice for the removal of iopamidol while *UV*/ClO_2 was the most reluctant one. The degradation rate in *UV*/Cl_2 was up to 4.45 times faster than that in *UV*/ClO_2. As for the application convenience, *UV*/Cl_2 also displayed great advantages on prices and accessibility of chemicals, specially considering the in situ preparation of ClO_2 in water works. Of course, more influence factors other than degradation efficiency should be taken into account in applying these *UV*-induced AOPs.

3.2. Degradation of iopamidol by four UV-induced AOPs

The degradation of iopamidol by four *UV*-induced AOPs were comprehensively investigated in terms of oxidant dosage, *UV* intensity, solution pH and water matrixes (Cl^-, NH_4^+ and NOM). The results obtained were plotted in Figs. 2–5 and Figs. S4–S11 applying the pseudo-first-order kinetics discussed in Section 3.1. The calculated k_{obs}, $t_{1/2}$ (half-life) and the determination coefficient (R^2) were shown in Figs. S4–S11 and Tables S6–S9 for comparison. Each curve was comprised of at least six experimentally data and the respective R^2 values were relatively high ($R^2 > 0.95$) to give enough analytical accuracy. The data might provide useful referential information for applications of the *UV*-mediated AOPs technologies relating to operational parameters as oxidant dosage, *UV* intensity, pH and water matrixes.

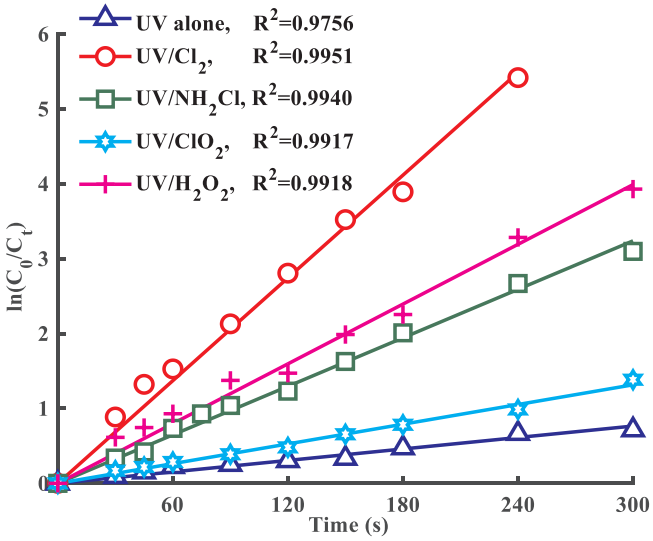

Fig. 1. Pseudo-first-order kinetics plot of iopamidol by different *UV*-based processes ([iopamidol]$_0$ = 10 μM, [phosphate buffer] = 10 mM, *UV* intensity = 2.43 mW cm^{-2}, [Cl_2] = [NH_2Cl] = [ClO_2] = [H_2O_2] = 200 μM).

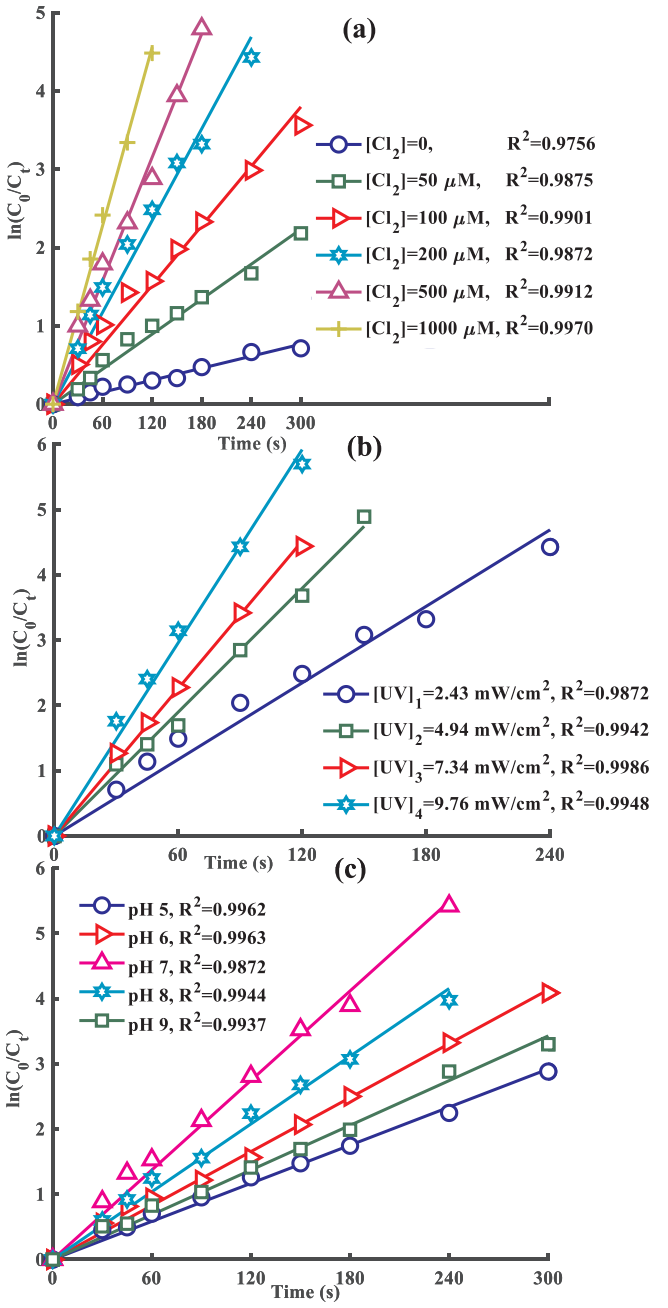

Fig. 2. Pseudo-first-order kinetics plot of iopamidol during *UV/Cl₂* process with different *Cl₂* dosages (a), *UV* intensity (b) and solution pH (c) ([iopamidol]$_0$ = 10 μM, [phosphate buffer] = 10 mM).

3.2.1. Degradation of iopamidol by UV/Cl₂ process

The *UV/Cl₂* degradation of iopamidol with different influencing factors was plotted in Fig. 2 and S4-S5. The reactive radicals and related reactions included in *UV/Cl₂* were summarized in Table S2. k_{obs}, $t_{1/2}$ and iopamidol degradation after 300 s reaction under different conditions were provided in Table S6.

As shown in Fig. 2(a) and S4(a), increasing *Cl₂* concentrations from 0 to 1000 μM resulted in substantial enhancement of k_{obs}. Since the increase of *Cl₂* concentrations led to higher productions of radical species towards iopamidol [26,27], the observed positive correlation between *Cl₂* dosages and the removal rate can be expected. But the degradation role of ·*OH* was not sensitive to *Cl₂* dosages. In fact, during the *UV/Cl₂* degradation of micropollutants, Wu et al. have proved that the concentration of ·*OH* almost kept unchanged as *Cl₂* dosages added,

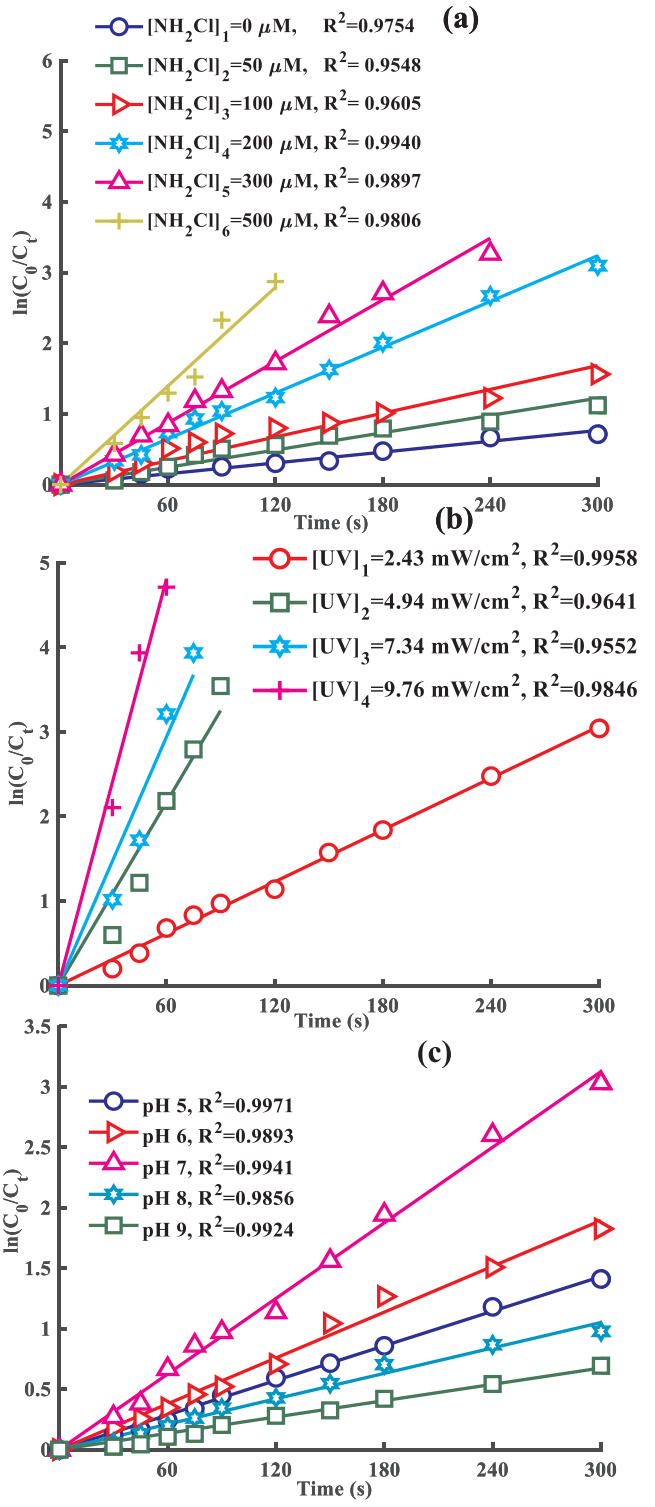

Fig. 3. Pseudo-first-order kinetics plot of iopamidol during *UV/NH₂Cl* process with different *NH₂Cl* dosages (a), *UV* intensity (b) and solution pH (c) ([iopamidol]$_0$ = 10 μM, [phosphate buffer] = 10 mM).

but that of *Cl*· increased linearly and that of *ClO*· added with the increasing rate gradually slowed down [27]. It is the added RCS that contributed to the faster removal of iopamidol at higher *Cl₂* doses. The conclusion coincided with other scholars' findings [18,26,27].

As given in Fig. 2(b) and S4(b), the degradation rate of iopamidol increased remarkably with *UV* intensity, from which the fine linearity between k_{obs} and *UV* intensity can be inferred (R^2 = 0.9079, the fitting

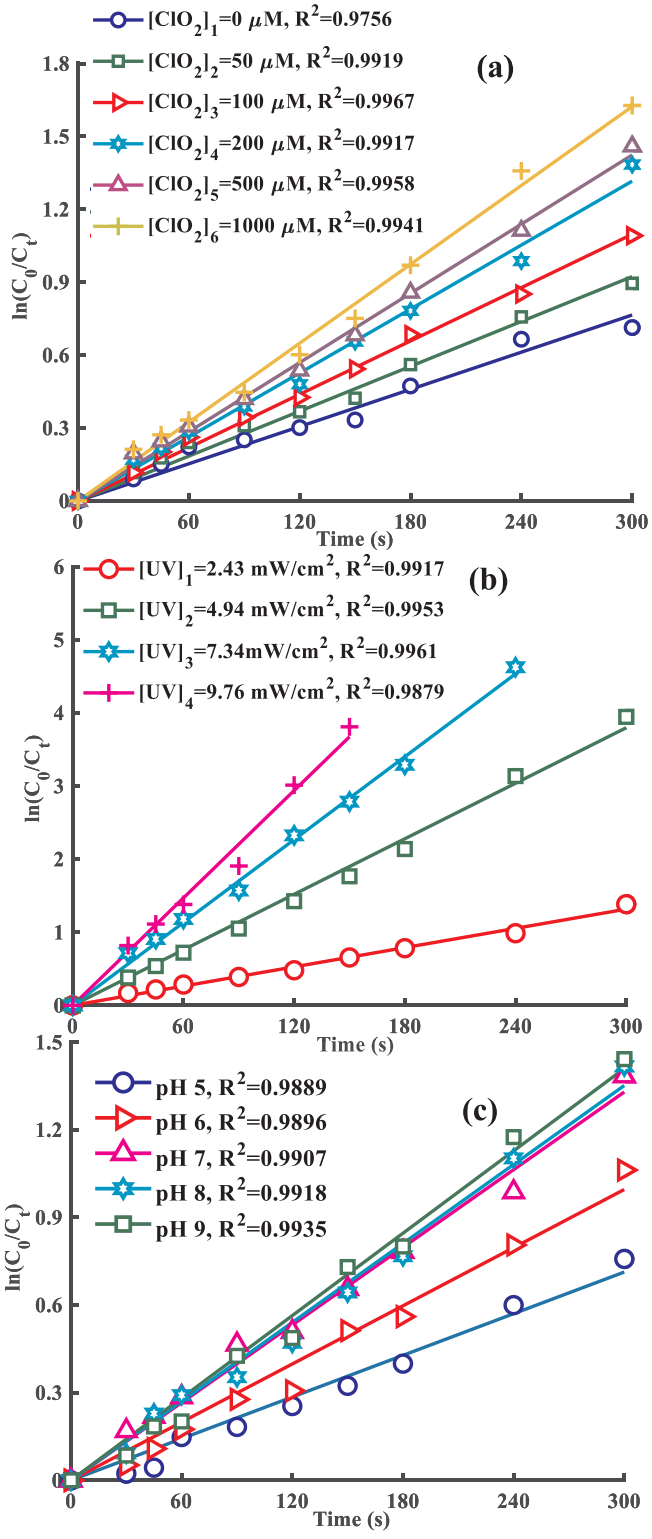

Fig. 4. Pseudo-first-order kinetics plot of iopamidol during UV/ClO_2 process with different ClO_2 dosages (a), UV intensity (b) and pH (c) ([iopamidol]$_0$ = 10 μM, [phosphate buffer] = 10 mM).

line was k_{obs} = 0.00545 [UV]). This stated the vital role of UV intensity in the UV/Cl_2 degradation of iopamidol. The results can be attributed to the increased degradation contributions of both radicals (including RCS and $\cdot OH$) and UV photolysis (Eq. (2)) at higher UV intensities.

The influence of pH on the UV/Cl_2 degradation of iopamidol was supplied in Fig. 2(c) and S4(c). It seemed that pH conditions had a great

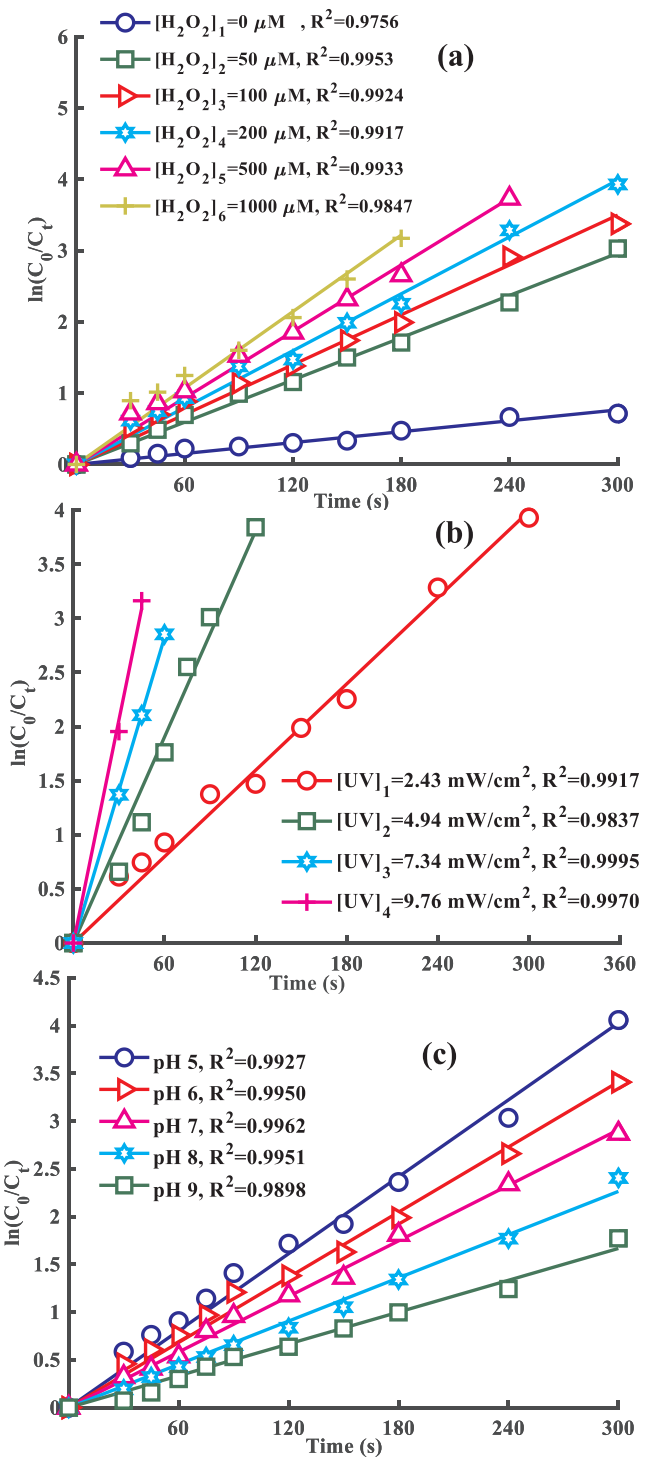

Fig. 5. Pseudo-first-order kinetics plot of iopamidol during UV/H_2O_2 process with different H_2O_2 dosages (a), UV intensity (b) and solution pH (c) ([iopamidol]$_0$ = 10 μM, [phosphate buffer] = 10 mM).

influence on the degradation rate of iopamidol. Among the inquired pHs, the highest k_{obs} appeared at pH 7. The data were distinct from other scholars which reported that the highest reactivity towards pollutants in UV/Cl_2 exhibited at low pHs, where $\cdot OH$ was the dominant radical contributor to the degradation [26,27,60,61]. Kong et al. have demonstrated that it is the indirect radicals ($Cl_2\cdot^-$ and $ClO\cdot$) not primary radicals ($\cdot OH$ and $Cl\cdot$) were responsible for the degradation of iopamidol at pH 7 [18]. The k_{obs} rank of pH behavior was pH 7 > pH 8 > pH 6 > pH 9 > pH 5. Solution pH can greatly affect the

dissociation of *HOCl* (reaction (6) in Table S2). The formations of $Cl\cdot$ and $\cdot OH$ were reduced as pH increased because of the weakened photolysis of chlorines and the enhanced radical scavenging [27]. The decreased k_{obs} as pH fluctuated around 7 can be ascribed to the combined consequence of the declined radical productions and the simultaneous consumption of $\cdot OH$ by OH^- (reaction (3) in Table S2) [18].

The effect of water matrixes (Cl^-, NH_4^+ and NOM) on the UV/Cl_2 oxidation of iopamidol was plotted in Fig. S5. The presence of Cl^-displayed negligible effect on the degradation rate, because the concentrations of $OH\cdot$ and $Cl\cdot$ were reported to be constant with Cl^- present [17]. Besides, the concentrations of Cl^- tested did not affect the species distributions of ClO^- [17,18]. The degradation of iopamidol was greatly inhibited by the appearance of NH_4^+ (Fig. S5(b)), but the inhibition was not correlated with the NH_4^+ concentrations. This can be attributed to the reaction of NH_4^+ and ClO^- to form chloramines, yet the yields of chloramines posed negligible influence on the degradation rate [27]. Meanwhile, as Fig. S5(c) listed, the presence of NOM in real waters also exhibited certain inhibitory effect on the UV/Cl_2, degradation of iopamidol, as NOM could act as inner filter of *UV* and scavenger of reactive radicals as well as ClO^- [17]. Furthermore, the degradation of iopamidol in the presence of NOM can not be described by the pseudo-first-order model. So the degradation curves were given instead of linear fitting plots.

The findings of this part indicated that UV/Cl_2 was an emerging alternative AOPs for the removal of iopamidol. The decomposition of iopamidol was favorable to higher Cl_2 dosages and *UV* intensities as well as neutral pH conditions. Cl^- showed negligible effect while NH_4^+ and NOM exhibited inhibitory effect on the degradation of iopamidol. But the highly reactive RCS in UV/Cl_2 might lead to diverse intermediates as the major mechanisms may not be the *Cl*-substitution and RCS were inclined to attack organics by the electron transport instead of H-abstraction and addition in comparison with $\cdot OH$ [18,62]. The oxidation of these intermediates in subsequent disinfection might pose non-ignorable toxicity effect on the treated waters.

3.2.2. Degradation of iopamidol by UV/NH_2Cl process

The UV/NH_2Cl degradation of iopamidol with different influencing factors was shown in Fig. 3 and S6–S7. The involved radicals and related reactions included in UV/NH_2Cl were sorted in Table S3. k_{obs}, $t_{1/2}$ and iopamidol degradation after 300 s reaction under different conditions were provided in Table S7.

As shown in Fig. 3(a) and S6(a), the synergistic degradation of iopamidol may result from the formation of $\cdot OH$ and $\cdot Cl$ in solution [23], and the productions of these species were promoted as the concentrations of NH_2Cl added. However, the relevant rate growth slowed down obviously. This could be attributed to the transformation of primary radicals to nitrogen-containing radicals ($NH_2\cdot$ and $NHCl\cdot$, etc), which was considered to have lower oxidative capacity and could be ignored in the degradation of iopamidol (reactions (2), (5) (10) and (12) in Table S3) [23,30,63]. Moreover, chloramines could also eliminate $\cdot OH$ and the reaction was more easily to occur than that between $\cdot OH$ and *HClO* (reactions (5) and (12) in Table S3) [30,64]. The results were consistent with previous studies [23,31].

The data in Fig. 3(b) showed that the degradation rate of iopamidol was distinctly improved as *UV* intensity added. As depicted in Fig. S6(b), the linear correlation between k_{obs} and *UV* intensity was obtained (R^2 = 0.9419, the fitting line was $k_{obs} = 0.007609\,[UV]$), which stated the critical significance of *UV* intensity. As *UV* intensity enhanced, the radicals ($Cl\cdot$, $\cdot OH$ and $NHCl\cdot$, etc.) originated from the decomposition of NH_2Cl increased, and the simultaneous *UV* photolysis was also intensified. The dual action upon iopamidol resulted in the higher k_{obs}. The radicals contributed as high as 76.35% to the total degradation in UV/NH_2Cl (Fig. 1). The increase of *UV* intensity provided much more reactive radicals and *UV* photons to iopamidol degradation. The results agreed well with former reports [30,65].

The pH behavior of UV/NH_2Cl degradation upon iopamidol was provided in Fig. 3(c) and S6(c). It was observed that solution pH also displayed a significant effect on the degradation rate. The highest k_{obs} in the pH range of 5–9 appeared at pH 7, which was consistent with that of UV/Cl_2 system. This might be ascribed to the homologous radicals of $\cdot OH$ and $\cdot Cl$ in both processes [32,66–68]. k_{obs} followed the order of pH7 > pH6 > pH5 > pH8 > pH9 and the tendency was slightly different from that in UV/Cl_2. The phenomena may be explained by the self-degradation of NH_2Cl and the equilibrium transfer of various chloramine forms (reactions (13)-(16) in Table S3 during the variation of pH [69,70]. Besides, OH^- could consume $\cdot Cl$ at higher pHs more quickly (reaction (2) in Table S3) [16]. Our previous reports have confirmed that the chloramination of iopamidol was also based on the action of free chlorines (*HOCl* and ClO^-, especially the more reactivie ClO^- towards iopamidol) from the NH_2Cl dissociation [57]. Under alkaline conditions, the self-degradation of NH_2Cl (reaction (16) in Table S3) shifted to the right, resulting in great inhibition to reaction (15) in Table S3. At the acidic pHs, the main chloramine species were $NHCl_2$ and reaction (13) in Table S3 shifted leftward, thus the k_{obs} were higher than those in alkaline solutions. The consequences were caused by both transformation of chlorine species and equilibrium of *HOCl* and ClO^-. This may be interpreted by the most production of ClO^- at neutral pH, while at pH 5–6 and pH 8–9, the conversion to ClO^- was greatly restrained, so the k_{obs} decreased obviously.

The effect of water matrixes including Cl^-, NH_4^+ and NOM on the UV/NH_2Cl degradation of iopamidol was plotted in Fig. S7. As depicted in Fig. S7, no significant difference of k_{obs} was observed among different concentrations of Cl^- as well as NH_4^+ and it seemed that the degradation rate was not affected by the presence of both Cl^- and NH_4^+. However, the degradation of iopamidol was markedly inhibited with the addition of NOM, which might be due to the consuming competion of NOM towards the indirect free chlorines and then radicals of $\cdot OH$ and $\cdot Cl$.

The results of this section suggested that the UV/NH_2Cl degradation rate of iopamidol could be accelerated with higher NH_2Cl dosages and *UV* intensities or adjusting pH to near-neutral conditions. The presence of both $Cl^-$and NH_4^+ showed negligible influence on the degradation rate but NOM exhibited distinctly inhibitory effect. Nevertheless, the nitrogen-containing radicals during the *UV* excitation of NH_2Cl might participate in the subsequent reaction towards the intermediates of the parent compound and thus result in other health risks to the treated waters, for example, the inclined formation of much more toxic nitrogen-containing DBPs.

3.2.3. Degradation of iopamidol by UV/ClO_2 process

The degradation of iopamidol by UV/ClO_2 with different influencing factors was shown in Fig. 4 and S8–S9. The reactive radicals and related reactions included in UV/ClO_2 were listed in Table S4. k_{obs}, $t_{1/2}$ and iopamidol degradation after 300 s reaction under different conditions were provided in Table S8.

As shown in Fig. 4(a) and S8(a), k_{obs} increased with the increasing ClO_2 concentrations from 0 to 1000 μM due to the added yields of radicals. Although UV/ClO_2 showed the least additive effect in the degradation rate compared with other *UV*-based AOPs, the roles of radicals were also nonnegligible in this system. The formation of $\cdot OH$ has been proposed in UV/ClO_2 assisted decolorization of methylene blue as well as color and chemical oxygen demand removal [50,52]. As listed in Table S4, two distinctive photodissociation channels have been suggested (reactions (1)–(2)) [71–73], the newly generated $O(^1D)$ atom may combine with atmospheric O_2 to reform O_3 (reaction (4)) [74] and react fast with H_2O to produce $\cdot OH$ (reaction (7)) [75]. But according to the data here, the radical yields were too low to present an outstanding promotion on the degradation rate. The formation of highly energetic $\cdot O$ and O_3 in UV/ClO_2 might influence the oxidation mechanisms of iopamidol and then lead to totally different oxidation products in comparison with those in UV/Cl_2.

As illustrated in Fig. 4(b) and S8(b), the UV/ClO_2 degradation rate of iopamidol increased linearly with UV intensity, the fitting line of which can be deduced as $k_{obs} = 0.00252\,[UV]$ ($R^2 = 0.9856$). Greater k_{obs} was obtained at higher UV intensities, because photons and radicals attacking the triiodinated compound increased with the number of photons entering into the iopamol samples added. This result was in accordance with the published studies [50–52].

The pH impact on k_{obs} was also evaluated in the range of 5–9 and displayed in Fig. 4(c) and S8(c). The degradation rate gradually increased with solution pH but the k_{obs} added limitedly with pH ascending from 7 to 9. The higher k_{obs} were noticed under neutral and basic media at pH 7–9 but decreased in acidic media at pH 7–5. Our previous study has confirmed that pH can not affect the UV photolysis rate of iopamidol and there is no dissociated form of iopamidol at all investigated pHs [15]. Such pH behavior here might be the integrated degradation results of multi-radicals as $\cdot OH$, $\cdot O$, $Cl\cdot$ and $ClO\cdot$, especially the highly reactive RCS, the reactivity of which was inhibited in acidic conditions [18]. For example, the k_{obs} at pH 5 was calculated to be 0.002377 s^{-1}, which implied the negligible contribution of radicals in UV/ClO_2 with UV photolysis alone calculated to be 0.002551 s^{-1}. The present results were in accord with the published literature on UV/ClO_2 decolorizing of azure C dye [51].

The influence of water matrixes (Cl^-, NH_4^+ and NOM) was provided in Fig. S9. It can be concluded that Cl^- slightly accelerated the degradation rate while NH_4^+ resulted in noticeable promotions of k_{obs}, while the effect of NOM can be neglected. The presence of Cl^- might induce a series of reactions by $\cdot OH$ (reactions (12)–(17) in Table S2), which finally led to the formation of more reactive $Cl\cdot$ and $Cl_2\cdot^-$ towards iopamidol. Although the transformation of $\cdot OH$ to RCS was quite limited, the promotions of degradation rate can be observed. Studies has demonstrated that NH_3/NH_4^+ could be oxidized to NO_2^- and NO_3^- by $\cdot OH$ (reactions (5)–(15)), then the generation of $\cdot O$ from the UV photo-reduction of NO_3^- (reactions (16)–(18)) [76–77]. The highly reactive $\cdot O$ might be responsible for the enhanced degradation.

$$NH_4^+ + H_2O \rightarrow NH_3 + H_3O^+ \; pka = 9.246 \quad (5)$$

$$NH_3 + \cdot OH \rightarrow NH_2\cdot \;\; k = 1 \times 10^8 M^{-1}s^{-1} \quad (6)$$

$$NH_2\cdot + \cdot OH \rightarrow NH_2OH \;\; k = 9.5 \times 10^9 M^{-1}s^{-1} \quad (7)$$

$$NH_2\cdot + O_2 \rightarrow NH_2O_2\cdot \; k = 3 \times 10^8 M^{-1}s^{-1} \quad (8)$$

$$NH_2OH + \cdot OH \rightarrow \cdot NHOH + H_2O \quad k = 9.5 \times 10^9 M^{-1}s^{-1} \quad (9)$$

$$NH_2O_2\cdot + \cdot OH \rightarrow HNO_2 + H_2O \quad (10)$$

$$NH_2O_2\cdot \rightarrow \cdot NO + H_2O \quad (11)$$

$$\cdot NO + \cdot OH \rightarrow HNO_2 \;\; k = 8.9 \times 10^9 M^{-1}s^{-1} \quad (12)$$

$$NO_2^- + \cdot OH \rightarrow \cdot NO_2 + OH^- \; k = 1.1 \times 10^{10} M^{-1}s^{-1} \quad (13)$$

$$\cdot NO_2 + \cdot OH \rightarrow NO_3^- + H^+ \;\; k = 1 \times 10^{10} M^{-1}s^{-1} \quad (14)$$

$$2\cdot NO_2 + H_2O \rightarrow NO_2^- + NO_3^- + H^+ \; k = 6.5 \times 10^7 M^{-1}s^{-1} \quad (15)$$

$$NO_3^- + h\nu \rightarrow \cdot NO_2 + O\cdot^- \quad (16)$$

$$O^-\cdot + H_2O \rightarrow \cdot OH + OH^- \; k = 1.8 \times 10^6 M^{-1}s^{-1} \quad (17)$$

$$NO_3^- + h\nu \rightarrow NO_2^- + O\cdot \quad (18)$$

The findings stated that the removal of iopamidol can be achieved by the combination of UV and ClO_2 and the degradation rate was favorable to higher ClO_2 dosages and UV intensities as well as basic pHs. The presence of Cl^- and NH_4^+ in UV/ClO_2 can clearly promote k_{obs} while the effect of NOM can be neglected. Although the radicals generated in UV/ClO_2 were partly similar to those in UV/Cl_2, k_{obs} of the former was far smaller. The difference might lead to quite different degradation pathways and intermediates, which could affect the formation of toxic DBPs in subsequent disinfection. The destruction mechanisms of UV/ClO_2 on contaminants still need further investigations.

3.2.4. Degradation of iopamidol by UV/H_2O_2 process

The degradation of iopamidol by UV/H_2O_2 with different influencing factors was shown in Fig. 5 and S10–S11. The reactive radicals and related reactions included in UV/H_2O_2 were summarized in Table S5. k_{obs}, $t_{1/2}$ and iopamidol degradation after 300 s reaction under different conditions were provided in Table S9.

As depicted in Fig. 5(a) and S10(a), the data suggested that the elimination rate of iopamidol (k_{obs}) gradually increased with added H_2O_2 dosage but the relationship was not linear. The results can be ascribed to the increased radicals (Table S5, mainly referring to $\cdot OH$) in solution at higher H_2O_2 dosages upon the same UV intensity. This conclusion was consistent with the published reports [18].

As shown in Fig. 5(b) and S10(b), the degradation rate of iopamidol increased remarkably with UV intensity. It can also be seen that k_{obs} was directly proportional to UV intensity and the good linear fits can be observed ($R^2 = 0.9842$, the fitting equation as $k_{obs} = 0.0067367\,[UV]$), the relationship of which suggested the critical importance of UV intensity. Much more radicals can be generated at higher UV intensities by the enhanced photolysis of H_2O_2 [35,56]. Furthermore, UV photolysis alone contributed 19.18% of the total iopamidol degradation in UV/H_2O_2 (Fig. 1). The joint action of both aspects led to the promoted k_{obs} at higher UV intensities. The results agreed broadly with previous studies by other scholars [54,56].

The pH effect on the UV/H_2O_2 degradation of iopamidol was plotted in Fig. 5(c) and S10(c). The k_{obs} distinctly decreased with pH increasing from 5 to 9. The increasing OH^- in alkaline conditions caused the consumption of $\cdot OH$ and the simultaneous formation of $O^-\cdot$ (reactions (9) and (10) in Table S5) [78]. It is supposed that $\cdot OH$ acts as electrophile while $O^-\cdot$ behaves as nucleophile in their respective reaction with organic molecules [79]. So as pH increased, the less reactive and more selective radical of $O^-\cdot$, rather than $\cdot OH$, became the major radical towards iopamidol [59,79], which then displayed a tardy degradation rate. Besides, the I^- originated from the UV deiodination also slightly inhibited the removal of iopamidol [17]. These dual effects resulted in a distinct decrease of k_{obs} under basic pHs. The pH behavior here was in correspondence with other relative reports [17,18].

The effect of water matrixes of Cl^-, NH_4^+ and NOM on the UV/H_2O_2 degradation of iopamidol was given in Fig. S11. It was seen from Fig. S11 that Cl^- showed slightly enhancement on k_{obs} while NH_4^+ resulted in obvious accelerations. The explanations could also be attributed to the formation of RCS and $\cdot O$, which were initiated by $\cdot OH$, as discussed in Section 3.2.3. Besides, NOM displayed weakly inhibitory effect on the degradation rate as the organic matter present in real waters interfered with the photooxidation of iopamidol.

The results of this section revealed that the promotion of UV/H_2O_2 degradation rate of iopamidol could be realized by enhancing H_2O_2 dosages and UV intensities or adjusting pH to acidic conditions. The occurrence of Cl^- and NH_4^+ can also noticeably promote k_{obs} while NOM exhibited slight inhibition. Utilization of greater UV intensity can be a preferred operation with more facility. However, these measures might also greatly improve the prime cost of this technology. In actual operation, it can be applied flexibly under full cost-effective assessment.

3.3. Energy calculations

As discussed above, the removal effectiveness and major factors of different UV-driven AOPs on iopamidol were investigated comprehensively. As all these photodegradation processes are electric-energy-intensive, it is necessary to introduce a scale-up parameter correlated with the electric energy, which can represent a primary fraction of the operating costs with regard to these techniques [25,80]. Therefore, the concept of EE/O proposed by the international union of pure and applied chemistry (IUPAC) was then employed to provide a cost-effective

evaluation for the concerned systems [81]. *EE/O* (kWh m^{-3} $order^{-1}$) is defined as the electrical energy (kWh) required to decompose the contaminants by one order magnitude in 1 m^3 of polluted water [25,81,82]. The whole *EE/O* is constituted by the electrical energy from *UV* light (EE/O_{uv}) and the equivalent electrical energy for oxidant consumption ($EE/O_{oxidant}$), values of which can be calculated by Eqs. (19)–(21) [81,83].

$$EE/O = EE/O_{UV} + EE/O_{oxidant} \quad (19)$$

$$EE/O_{UV} = \frac{P \times t \times 1000}{V \times \log \frac{C_0}{C_t}} \quad (20)$$

$$EE/O_{oxidant} = Eq_{oxidant} \times \frac{[oxidant] \times 1000}{\log \frac{C_0}{C_t}} \quad (21)$$

where P represents power of the electronic energy input of the *UV* device (kW, as listed in Text S2); V is the volume of the solution (L); t is the photodegradation time (h); [oxidant] means the utilized dosages of oxidant (mol L^{-1}); $\log \frac{C_0}{C_t}$ is the logarithm of the initial and instant concentrations of the contaminant; k_{obs} is the pseudo-first-order rate constant of the iopamidol degradation (s^{-1}); $Eq_{oxidant}$ is the electric energy consumption to generated per mole of oxidant equivalently (Eq_{Cl_2} = 1.6210 kWh mol^{-1}, Eq_{ClO_2} = 3.452 kWh mol^{-1}, Eq_{NH_2Cl} = 1.3900 kWh mol^{-1}, $Eq_{H_2O_2}$ = 0.3586 kWh mol^{-1}, the calculations of the unit conversion were detailed in Text S2). Then the calculated values and compositions of *EE/O* for iopamidol degradation by different *UV*-based processes were shown in Fig. S2 and Tables S6–S9.

As shown in Fig. S2, k_{obs} followed the order of UV/Cl_2 > UV/H_2O_2 > UV/NH_2Cl > UV/ClO_2 > *UV*. However, the total *EE/O* followed the almost contrary trend of UV/ClO_2 > *UV* > UV/NH_2Cl > UV/H_2O_2 > UV/Cl_2. As *EE/O* increases, the energy efficiency of a system decreases [84]. UV/Cl_2 was observed to be the most cost-effective one for iopamidol degradation among the tested AOPs. Contrarily, UV/ClO_2 was the highest energy consumption system owing to the biggest equivalent electrical energy of ClO_2 and the lowest degradation rate. Compared with direct *UV* photolysis, EE/O_{UV} decreased obviously in the discussed processes due to the contribution of various radical species in k_{obs}. EE/O_{UV} dominated the total *EE/O*, which proved the significant role of *UV* intensity in all of these *UV*-mediated AOPs.

As presented in Tables S6–S9, the necessary *UV* energy (EE/O_{UV}) decreased with the growing oxidant dosages, while the $EE/O_{oxidant}$ increased instead. Then the proportions of EE/O_{UV} and $EE/O_{oxidant}$ changed accordingly. The optimal oxidant dosages in UV/Cl_2, UV/NH_2Cl, UV/ClO_2 and UV/H_2O_2 for their lowest *EE/O* values were estimated at 200, 300, 100 and 200 μM, respectively, which corresponded to the *UV* intensity of 2.43 mW cm^{-2}. With the increased *UV* intensity, the total *EE/O* reduced gradually in UV/NH_2Cl, UV/ClO_2 and UV/H_2O_2 but obviously added in UV/Cl_2. This indicated that it is unnecessary to enhance *UV* intensity in the UV/Cl_2 degradation of iopamidol when taking into consideration of energy optimization. Under specific *UV* intensity and oxidant dosage with different pHs, the minimum of *EE/O* appeared where k_{obs} reached its maximum in each process. The results of current study can provide a few usefully cost-effective concerns in the application of these *UV*-driven AOP technologies.

3.4. DBPs-related toxicity evaluation in sequential disinfection processes

It can be concluded from the above results that the four *UV*-induced AOPs were all capable of degrading iopamidol effectively compared with *UV* alone. Our previous research has confirmed the formation of I^- released from iopamidol and its intermediates during *UV* irradiation, which then resulted in an enhanced conversion of classical DBPs to highly toxic I-DBPs during subsequent oxidation [15]. Other scholars have also verified deiodination as the vital pathways and the evolution of inorganic iodine (I^- and HOI) in the degradation of iopamidol by UV/H_2O_2 and UV/Cl_2 [17,18]. The I^- present in these *UV* based systems can be oxidized to *HOI*, which further reacted with degradation intermediates of iopamidol and probably led to the formation of undesirable I-DBPs [13,15,17].

The organic oxidation products of iopamidol by *UV*, UV/H_2O_2 and UV/Cl_2 have been identified and the destruction mechanisms mainly include deiodination, hydroxylation, chlorination and H-abstraction [15,17,18]. The degradation intermediates of iopamidol by UV/Cl_2, UV/NH_2Cl, UV/ClO_2 and UV/H_2O_2 were also analyzed here and the results were shown in Table S11 and Fig. S12. It was seen that the deiodinated and hydroxylated products were all detected in the four processes. The chlorinated products were both observed in UV/Cl_2 and UV/NH_2Cl, while chlorine substitutions and hydroxy substitutions of iodine atoms might simultaneous take place, which resulted in much more intermediates than other two systems. The detected products of UV/ClO_2 and UV/H_2O_2 were similar except for slight monochlorinated products (products 8 and 12 in Table S11). It should also be pointed out that amino group substituted products (such as product 2 in Table S11) were noticed in UV/NH_2Cl, which might pose serious influence on the formation of nitrogen- containing DBPs. These oxidized intermediates can provide sufficient organic carbon source and may then facilitate the subsequential attack by oxidants to form DBPs.

The main parameters (TOC, TN and UV_{254}) of iopamidol solutions after treated by different processes were presented in Table S10. It can be seen that removals of TOC and UV_{254}, which both decreased in the order of UV/Cl_2 > UV/H_2O_2 > UV/ClO_2 > *UV* > UV/NH_2Cl, were little though there were radicals within all systems. The TOC data provided valuable information on the mineralization extent of samples. The results can be explained by the fact that the reactivity of radicals was firstly consumed by iopamidol and its derivates, while the irradiation time was not enough to realize the distinct conversion of these compounds to plant accessible forms, i.e., CO_2, H_2O, NH_3/NH_4^+ or NO_3^-. UV_{254} is an optical parameter indicating the chromophores with conjugated double bond functional groups (C═O, C═C, C═N) and aromatic rings of dissolved organic matter in solution [46]. Scholars have revealed that RCS were prone to attack aromatics containing hydroxyl or amino groups while ·*OH* mainly led to deiodination and addition reactions [17,18]. The results of TOC and UV_{254} evidenced reactivities of RCS and ·*OH* in the respective system. Besides, the changes of TN were not notable in all samples except that of UV/NH_2Cl, the sharp increase of which could be ascribed to reactions of nitrogen-containing radicals (NH_2· and *NHCl*·, etc).

The variations of these parameters in each sample indicated the reactivity features of these *UV*-based AOPs and may pose different effects on DBPs formation. The distinct reactivity of radicals resulted in varied oxidation products by deiodination, hydroxylation, chlorination and H-abstraction, etc. Thus the DBPs-related toxicity of waters in subsequent oxidation processes might display quite differently. Nevertheless, the influence of these processes on the DBPs formation and the solution toxicity during the subsequent disinfection are still unknown. This information has important indicative significance in evaluating the application of these technologies. Therefore, investigations on the formation of classical DBPs and I-THMs during various *UV*-based AOPs and sequential disinfection of iopamidol were carried out and the results were exhibited in Fig. 6. To facilitate comparison, the total production of classical DBPs and I-THMs as well as the iodine conversion of iopamidol to I-THMs were also calculated in Table S12.

As seen from Fig. 6, five classical DBPs (including TCM, DCAN, TCAN, TCAL and TCNM) and three I-THMs (including DCIM, CDIM and TIM) were detected. It should be noted that certain amounts of nitrogen-containing DBPs (including DCAN, TCAN and TCNM) were observed. Though their concentrations were not remarkable, the corresponding impact on the toxicity of disinfected waters should not be ignored due to their higher toxicity than carbon-containing DBPs [85]. The attack of radicals in these systems led to the cleavage of asymmetric side chain at the amide bond of the hydroxylated products of

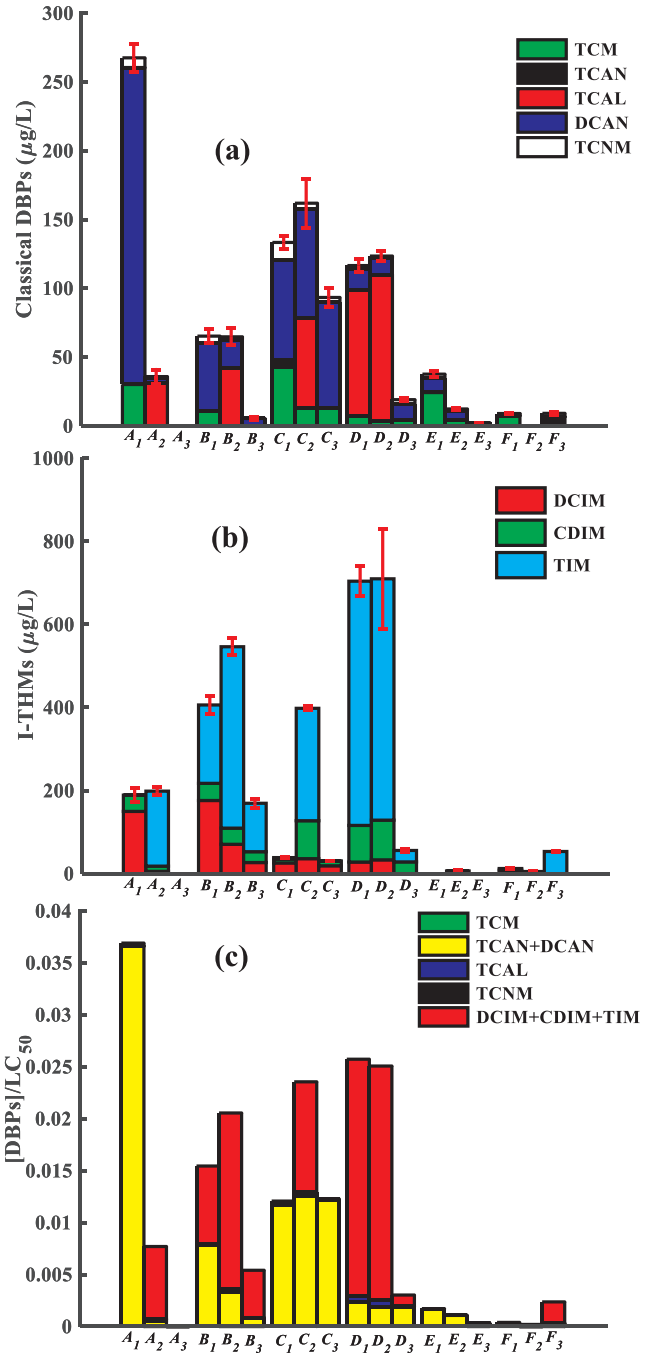

Fig. 6. Formation of classical DBPs (a), I-THMs (b) and the toxicity weighted concentrations of all DBPs measured during various *UV*-based AOPs of iopamidol (*UV* fluence = 1458 mJ cm^{-2}, pH = 7, [phosphate buffer] = 10 mM, $[iopamidol]_0$ = 10 μM, $[Cl_2]_0$ = $[NH_2Cl]_0$ = $[ClO_2]_0$ = $[H_2O_2]_0$ = 200 μM) followed by different disinfection processes (pH = 7, $[Cl_2]_0$ = $[NH_2Cl]_0$ = $[ClO_2]_0$ = 100 μM, t = 7 d). Error bars represent one standard deviation of triplicate measurements. Capital letters A, B, C, D, E and F indicate pretreatment by none, *UV* alone, *UV/Cl₂*, *UV/NH₂Cl*, *UV/ClO₂* and *UV/H₂O₂* processes, respectively, the subscript numbers 1, 2 and 3 represent subsequent oxidation by *Cl₂*, *NH₂Cl* and *ClO₂*, respectively.

iopamidol, and then formation of nitrogen-containing DBPs in the following oxidation [17]. The contribution of a certain DBP to the water toxicity after disinfection depends on its concentration as well as the toxic potency [86]. In order to better estimate the effects of various *UV*-combined AOPs on the toxicity of disinfected waters, the toxicity weighted concentrations of all tested DBPs were calculated and presented in Fig. 6(c) and Table S12.

In these five *UV*-activated systems, I^-could be released by *UV* deiodination of iopamidol [15]. However, the following reactions between I^- and various reactive species might result in the evolution of iodine speciation and thus affected the final formation of I-THMs in subsequent oxidation. The reaction rates of ROS and RCS towards iopamidol were quite different [17,18,87], and RCS were noticed to be more selective and efficient [17]. Consequently, the relevant products in subsequent reactions with I^- and the deiodinated intermediates of iopamidol differed greatly. The chlorinated intermediates of iopamidol by RCS were more liable to form I-THMs. On the contrary, ROS were more reluctant to induce I-THMs formation than RCS in the subsequent oxidation not only due to its reaction with I^- as reactions (22)-(23) but also the formation of hydroxylated products [79,87].

$$\cdot OH + 2I^- \rightarrow HOI^- \quad k = 1.1 \times 10^{10} M^{-1}s^{-1} \tag{22}$$

$$\cdot OH + I^- \rightarrow HOI\cdot^- \tag{23}$$

For the subsequent chlorination, these *UV*-based processes can repress the total formation of classical DBPs to some extent, but have different impact on the I-THMs formation. Pretreatment of iopamidol by these processes can considerably inhibit the DCAN formation, and thus dramatically reduced the overall toxicity of the solution, which showed the control effect of toxicity in the order as *UV/H₂O₂* > *UV/ClO₂* > *UV/Cl₂* > *UV* > *UV/NH₂Cl*. The sum production rank of classical DBPs was *UV/H₂O₂* < *UV/ClO₂* < *UV* < *UV/NH₂Cl* < *UV/Cl₂*, as expressed in Fig. 6(a) and Table S12. *UV/Cl₂* led to the greatest yields of classical DBPs, which may be attributed to its strongest oxidation ability towards iopamidol. This can also be evidenced by the fastest degradation rate (Fig. 1) and the most reduction of TOC as well as UV_{254} in *UV/Cl₂* (Table S10). Small molecular organic compounds present in *UV/Cl₂* were more beneficial to form classical DBPs during subsequent chlorination [89]. However, pretreatment by *UV* and *UV/NH₂Cl* resulted in a significant increase in the I-THMs formation, especially that by *UV/NH₂Cl* produced a large amount of TIM.

Meanwhile, *UV/H₂O₂* and *UV/ClO₂* induced only tiny amounts of I-THMs, which might owe to the reactions between different radicals and iodine species in these systems [63,64]. In *UV/H₂O₂*, both H_2O_2 and $\cdot OH$ can react with I^- (reactions (22)-(26)) [79,87], hence almost no I-THMs were detected in subsequent chlorination and chloramination (F_1 and F_2 in Fig. 6). It was probably due to the reactions of *Cl₂* and *NH₂Cl* with the iodine species as HOI^- and I_2. It should also be pointed out that certain amounts of TIM was detected in F_3, which may owe to the iodine active substances (*HOI*, I_2 and I_3^-) produced by the subsequent *ClO₂* oxidation (reactions (23), (27)-(28)) [79,88]. Besides, there were scarcely any I-THMs formed in *UV/ClO₂*. The O_3 produced by reaction (4) in Table S4 can easily oxidize I^- to IO_3^- (reaction (29)), thus the formation of I-THMs were completely restrained [11]. The iodine conversion of iopamidol to I-THMs (Table S12) increased in the order of *UV/NH₂Cl* > *UV* > *UV/Cl₂* > *UV/H₂O₂* > *UV/ClO₂*, which indicated the highest formation risk of I-THMs in *UV/NH₂Cl*.

$$H_2O_2 + e^-_{aq} \rightarrow \cdot OH + OH^- \quad k = 1.2 \times 10^{10} M^{-1}s^{-1} \tag{24}$$

$$H_2O_2 + 2I^- \rightarrow \cdot OH + I_2 + OH^- \tag{25}$$

$$H_2O_2 + 2I^- \rightarrow I_2 + 2OH^- \tag{26}$$

$$HOI\cdot^- \rightarrow I\cdot + OH^- \tag{27}$$

$$I\cdot + I^- \rightarrow I_2^-\cdot \tag{28}$$

$$3O_3 + I^- \rightarrow IO_3^- + 3O_2 \quad k = 2.0 \times 10^{9} M^{-1}s^{-1} \tag{29}$$

For the subsequent chloramination, much less TCM (the most common classical DBPs under control) was formed than that in chlorination. Nevertheless, the toxicity of waters was remarkably enhanced after chloramination due to the formation of more toxic TCAL, DCAN

and I-THMs in UV/NH_2Cl, UV/Cl_2 and UV. The occurrence of TCAL and DCAN were more susceptible to the oxidation by NH_2Cl [90,91]. Much more I-THMs (especially TIM) were formed in the following chloramination than chlorination, which was consistent with research results of other scholars [13,15]. As listed in Table S10, although UV/NH_2Cl slightly reduced TOC and UV_{254}, it resulted in sharp increase in TN, which consequently led to much more DCAN [92]. Besides, trace productions of classical DBPs and I-THMs were observed in UV/H_2O_2 and UV/ClO_2, which displayed minor toxicity in comparison with other three processes. The tendency of iodine conversion (Table S12) was similar to that in chlorination and UV/NH_2Cl should be avoided before both disinfection processes. The data also demonstrated that although all these UV-assisted AOPs can realize the removal of iopamidol, the systems dominated by ROS (UV/H_2O_2 and UV/ClO_2) seemed to have more advantages than those by RCS (UV/Cl_2 and UV/NH_2Cl) in controlling DBPs during subsequent oxidation. Therefore, when considering the control of DBPs, the ROS systems should be given much more attention. The results also revealed far greater disinfection risk of NH_2Cl than Cl_2, especially in I-THMs formation, which can provide referential value for the application of chlorine-based disinfectants.

It can also be seen from Fig. 6 that among three subsequent processes, ClO_2 produced the least DBPs, thus presented the smallest water toxicity. The data provided some evidences that ClO_2 could be a green disinfectant in controlling DBPs as Cl_2 and NH_2Cl alternatives [93]. ClO_2 alone could not oxidize iopamidol and produced none DBPs [15], but the pretreatment of UV-based processes induced a certain amount of DBPs. The iodine conversion to I-THMs followed the order of UV/NH_2Cl > UV/H_2O_2 > UV/Cl_2 > UV > UV/ClO_2, which clearly stated the elimination effect of UV/ClO_2 and the formation risk of UV/NH_2Cl. But the water toxicity descended in the order of UV/Cl_2 > UV > UV/NH_2Cl > UV/H_2O_2 > UV/ClO_2. Small molecular organic compounds in UV/Cl_2 were favored to form more DBPs in the subsequent ClO_2 oxidation thus engendered the most toxic conditions. Certain amounts of TCAN and TIM were detected in sequential treatment of UV/H_2O_2 and ClO_2, which resulted in a marked increase in DBPs-related toxicity compared with subsequent chlorination and chloramination. Besides, it should be specially pointed out that UV/ClO_2 can degrade iopamidol effectively with hardly any I-THMs formed during subsequent oxidation.

Up to present, iopamidol is reported to be the most important organic iodine source for I-DBPs [15,16,94] and the fate of iodine in iopamidol has critical significance in evaluating the relevant toxicity of waters. It was concluded that during the subsequent chlorination and chloramination, the iodine conversion in UV/NH_2Cl turned out to be the highest while those in UV/ClO_2 were quite low. As for the I-THMs-related safety in subsequent disinfection, the advantage of ClO_2 over Cl_2 and NH_2Cl was obviously noticed. The results can provide application value for these UV-induced techniques in treatment with iopamidol-contaminated waters as well as the toxicity control relating to I-THMs.

From the perspective of weighted water toxicity after subsequent oxidation, the risk ranking was UV/NH_2Cl > UV/Cl_2 > UV/H_2O_2 > UV/ClO_2. Based on our results, more concerns must be drawn in the utilization of UV/NH_2Cl and UV/Cl_2, UV/NH_2Cl in particular, as these treatments might greatly enhance the water toxicity in the following disinfection. In fact, ammonia nitrogen pollution in surface waters is generally serious while Cl_2 is the most widespread conventional disinfectant in most plants. Hence the safety issue concerning DBPs on the UV combination with NH_2Cl and Cl_2 should be addressed. Meanwhile, UV/ClO_2 displayed overwhelming advantage in controlling the water toxicity problems associated with DBPs, especially I-THMs, compared with other UV-driven AOPs.

4. Conclusions

The degradation of iopamidol by four UV-induced AOPs can be described by pseudo-first-order model. The calculated k_{obs} followed the order of UV/Cl_2 > UV/H_2O_2 > UV/NH_2Cl > UV/ClO_2 > UV. The synergistic effects could be attributed to different radical species generated by UV irradiation of oxidants. The removal rate of iopamidol was favorable to higher oxidant dosages and greater UV intensities. However, the pH behaviors of k_{obs} in these processes exhibited quite differently. The k_{obs} rank in UV/Cl_2 was pH7 > pH8 > pH6 > pH9 > pH5 while that in UV/NH_2Cl was pH7 > pH6 > pH5 > pH8 > pH9. k_{obs} in UV/ClO_2 gradually increased with solution pH whereas in UV/H_2O_2 it distinctly decreased. The effects of typical water matrixes including Cl^-, NH_4^+ and NOM on the degradation of iopamidol in these processes were also investigated. The concept of EE/O was employed here to provide a cost-effective evaluation for the tested AOPs and the constitutions of EE/O were then quantified. EE/O followed the trend of UV/ClO_2 > UV > UV/NH_2Cl > UV/H_2O_2 > UV/Cl_2. Pretreatment of iopamidol by UV/Cl_2 and UV/NH_2Cl clearly enhanced the formation of classical DBPs and I-THMs while UV/ClO_2 and UV/H_2O_2 exhibited almost elimination effect. From the perspective of weighted water toxicity, the risk ranking was UV/NH_2Cl > UV/Cl_2 > UV/H_2O_2 > UV/ClO_2. The results of current study can provide usefully cost-effective concerns and DBPs-related toxicity evaluation in the application of these UV-driven AOP technologies.

Declaration of Competing Interest

The authors declare that they have no known competing financial interests or personal relationships that could have appeared to influence the work reported in this paper.

Acknowledgments

This study was supported in part by the Natural Science Foundation of China (No. 51708353), Shuguang Program (No. 17SG52) by Shanghai Education Development Foundation and Shanghai Municipal Education Commission, the Science and Technology Program of Shanghai City of China (No. 16090503500). The authors would like to thank the anonymous reviewers for their valuable comments and suggestions to improve the quality of this paper.

Appendix A. Supplementary data

Supplementary data to this article can be found online at https://doi.org/10.1016/j.cej.2020.125570.

References

[1] J.T. Wu, K. Leung, G.M. Leung, Nowcasting and forecasting the potential domestic and international spread of the 2019-nCoV outbreak originating in Wuhan, China: a modelling study, Lancet (2020), https://doi.org/10.1016/S0140-6736(20)30260-9.

[2] Notice on Printing and issuing the diagnosis and treatment Plan for pneumonia caused by New Coronavirus infection (trial Fifth Edition), General Office of the State Health Commission and Office of the State Administration of traditional Chinese Medicine. http://www.nhc.gov.cn/yzygj/ s7653p/202002/3b09b894ac9b4204a79db5b8912d4440.shtml, 2020 (accessed 8 February 2020).

[3] S.D. Richardson C. Postigo Drinking water disinfection by-products 2011 Springer, Berlin, Heidelberg Emerging organic contaminants and human health 93 137.

[4] S.D. Richardson, M.J. Plewa, E.D. Wagner, R. Schoeny, D.M. DeMarini, Occurrence, genotoxicity, and carcinogenicity of regulated and emerging disinfection by-products in drinking water: a review and roadmap for research, Mutat. Res. 636 (2007) 178–242.

[5] S.W. Krasner, H.S. Weinberg, S.D. Richardson, S.J. Pastor, R. Chinn, M.J. Sclimenti, G.D. Onstad, A.D. Thruston, Occurrence of a new generation of disinfection by-products, Environ. Sci. Technol. 40 (2006) 7175–7185.

[6] S.D. Richardson, A.D. Thruston Jr, S.W. Krasner, H.S. Weinberg, R.J. Miltner, K.M. Schenck, M.G. Narotsky, A.B. McKague, J.E. Simmons, Integrated disinfection by-products mixtures research: comprehensive characterization of water concentrates prepared from chlorinated and ozonated/postchlorinated drinking water, J. Toxicol. Environ. Health Part A 71 (2008) 1165–1186.

[7] E. Cemeli, E.D. Wagner, D. Anderson, S.D. Richardson, M.J. Plewa, Modulation of the cytotoxicity and genotoxicity of the drinking water disinfection byproduct

iodoacetic acid by suppressors of oxidative stress, Environ. Sci. Technol. 40 (2006) 1878–1883.
[8] M.J. Plewa, E.D. Wagner, S.D. Richardson, A.D. Thruston, Y.T. Woo, A.B. McKague, Chemical and biological characterization of newly discovered iodoacid drinking water disinfection byproducts, Environ. Sci. Technol. 38 (2004) 4713–4722.
[9] M.J. Plewa, Y. Kargalioglu, D. Vankerk, R.A. Minear, E.D. Wagner, Mammalian cell cytotoxicity and genotoxicity analysis of drinking water disinfection by-products, Environ. Mol. Mutagen. 40 (2002) 134–142.
[10] Y. Kargalioglu, B.J. McMillan, R.A. Minear, M.J. Plewa, Analysis of the cytotoxicity and mutagenicity of drinking water disinfection by-products in Salmonella typhimurium, Teratog., Carcinog., Mutagen. 22 (2002) 113–128.
[11] Y. Bichsel, U. Von Gunten, Oxidation of iodide and hypoiodous acid in the disinfection of natural waters, Environ. Sci. Technol. 33 (1999) 4040–4045.
[12] D. Khiari, Distribution generated taste-and-odor phenomena, American, American Water Works Association, 2002.
[13] Y. Bichsel, U. Von Gunten, Formation of iodo-trihalomethanes during disinfection and oxidation of iodide-containing waters, Environ. Sci. Technol. 34 (2000) 2784–2791.
[14] S.L. des Eaux, Conditions de formation et destruction des trihalome' thane iode' s responsable des gouts et odeurs pharmaceutiques, Internal Report, Le 1993 Pecq, France.
[15] F.X. Tian, B. Xu, Y.L. Lin, C.Y. Hu, T.Y. Zhang, N.Y. Gao, Photodegradation kinetics of iopamidol by *UV* irradiation and enhanced formation of iodinated disinfection by-products in sequential oxidation processes, Water Res. 58 (2014) 198–208.
[16] S.E. Duirk, C. Lindell, C.C. Cornelison, J. Kormos, T.A. Ternes, M. Attene-Ramos, J. Osiol, E.D. Wagner, M.J. Plewa, S.D. Richardson, Formation of toxic iodinated disinfection by-products from compounds used in medical imaging, Environ. Sci. Technol. 45 (2011) 6845–6854.
[17] X. Zhao, J. Jiang, S. Pang, C. Guan, J. Li, Z. Wang, J. Ma, C. Luo, Degradation of iopamidol by three *UV*-based oxidation processes: Kinetics, pathways, and formation of iodinated disinfection byproducts, Chemosphere 221 (2019) 270–277.
[18] X. Kong, J. Jiang, J. Ma, Y. Yang, S. Pang, Comparative investigation of X-ray contrast medium degradation by *UV*/chlorine and *UV*/H_2O_2, Chemosphere 193 (2018) 655–663.
[19] T.A. Ternes, J. Stüber, N. Herrmann, D. McDowell, A. Ried, M. Kampmann, B. Teiser, Ozonation: a tool for removal of pharmaceuticals, contrast media and musk fragrances from wastewater? Water Res. 37 (2003) 1976–1982.
[20] M.N. Sugihara, D. Moeller, T. Paul, T.J. Strathmann, TiO_2-photocatalyzed transformation of the recalcitrant X-ray contrast agent diatrizoate, Appl. Catal. B 129 (2013) 114–122.
[21] Z. Wang, Y.L. Lin, B. Xu, S.J. Xia, T.Y. Zhang, N.Y. Gao, Degradation of iohexol by UV/chlorine process and formation of iodinated trihalomethanes during post-chlorination, Chem. Eng. J. 283 (2016) 1090–1096.
[22] Y.Q. Gao, N.Y. Gao, D.Q. Yin, F.X. Tian, Q.F. Zheng, Oxidation of the β-blocker propranolol by *UV*/persulfate: Effect, mechanism and toxicity investigation, Chemosphere 201 (2018) 50–58.
[23] L. Bu, S. Zhou, S. Zhu, Y. Wu, X. Duan, Z. Shi, D.D. Dionysiou, Insight into carbamazepine degradation by *UV*/monochloramine: reaction mechanism, oxidation products, and DBPs formation, Water Res. 146 (2018) 288–297.
[24] J. Iqbal, N.S. Shah, M. Sayed, N. Muhammad, S. Rehman, J.A. Khan, Z.U.H. Khan, F.M. Howari, Y. Nazzal, C. Xavier, S. Arshad, A. Hussein, K. Polychronopoulou, Deep eutectic solvent- mediated synthesis of ceria nanoparticles with the enhanced yield for photocatalytic degradation of flumequine under *UV*-C, J. Water Process Eng. 33 (2020) 101012.
[25] F. Rehman, M. Sayed, J.A. Khan, N.S. Shah, H.M. Khan, D.D. Dionysiou, Oxidative removal of brilliant green by *UV*/$S_2O_8^{2-}$, *UV*/HSO_5^- and *UV*/H_2O_2 processes in aqueous media: a comparative study, J. Hazard. Mater. 357 (2018) 506–514.
[26] L. Qin, Y.L. Lin, B. Xu, C.Y. Hu, F.X. Tian, T.Y. Zhang, W.Q. Zhu, H. Huang, N.Y. Gao, Kinetic models and pathways of ronidazole degradation by chlorination UV irradiation and UV/chlorine processes, Water Res. 65 (2014) 271–281.
[27] Z. Wu, K. Guo, J. Fang, X. Yang, H. Xiao, S. Hou, X. Kong, C. Shang, X. Yang, F. Meng, Factors affecting the roles of reactive species in the degradation of micropollutants by the *UV*/chlorine process, Water Res. 126 (2017) 351–360.
[28] X. Yang, J. Sun, W. Fu, C. Shang, Y. Li, Y. Chen, W. Gan, J. Fang, PPCP degradation by *UV*/chlorine treatment and its impact on DBP formation potential in real waters, Water Res. 98 (2016) 309–318.
[29] J. Jin, M.G. El-Din, J.R. Bolton, Assessment of the *UV*/chlorine process as an advanced oxidation process, Water Res. 45 (2011) 1890–1896.
[30] Y.H. Chuang, S. Chen, C.J. Chinn, W.A. Mitch, Comparing the *UV*/monochloramine and *UV*/free chlorine advanced oxidation processes (AOPs) to the *UV*/hydrogen peroxide AOP under scenarios relevant to potable reuse, Environ. Sci. Technol. 51 (2017) 13859–13868.
[31] S. Patton, W. Li, K.D. Couch, S.P. Mezyk, K.P. Ishida, H. Liu, Impact of the ultraviolet photolysis of monochloramine on 1, 4-dioxane removal: new insights into potable water reuse, Environ. Sci. Technol. 4 (2017) 26–30.
[32] C. Remucal, D. Manley, Emerging investigators series: the efficacy of chlorine photolysis as an advanced oxidation process for drinking water treatment, Environ. Sci. Water Res. Technol. 2 (2016) 565–579.
[33] Z. Zhang, Y.H. Chuang, A. Szczuka, K.P. Ishida, S. Roback, M.H. Plumlee, W.A. Mitch, Pilot-scale evaluation of oxidant speciation, 1, 4-dioxane degradation and disinfection byproduct formation during *UV*/hydrogen peroxide UV/free chlorine and UV/chloramines advanced oxidation process treatment for potable reuse, Water Res. 164 (2019) 114939.
[34] M.J. Watts, E.J. Rosenfeldt, K.G. Linden, Comparative *OH* radical oxidation using *UV*-Cl_2 and *UV*-H_2O_2 processes, J. Water Supply Res. Technol.-AQUA 56 (2007) 469–477.
[35] Y.S. Shen, Y. Ku, K.C. Lee, The effect of light absorbance on the decomposition of chlorophenols by ultraviolet radiation and *UV*/H_2O_2 processes, Water Res. 29 (1995) 907–914.
[36] M. Sörensen, S. Zurell, F. Frimmel, Degradation pathway of the photochemical oxidation of ethylenediaminetetraacetate (EDTA) in the *UV*/H_2O_2-process, Acta Hydrochim. Hydrobiol. 26 (1998) 109–115.
[37] R. Andreozzi, V. Caprio, A. Insola, R. Marotta, Advanced oxidation processes (AOP) for water purification and recovery, Catal. Today 53 (1999) 51–59.
[38] J.J. López-Peñalver, M. Sánchez-Polo, C.V. Gómez-Pacheco, J. Rivera-Utrilla, Photodegradation of tetracyclines in aqueous solution by using *UV* and *UV*/H_2O_2 oxidation processes, J. Chem. Technol. Biotechnol. 85 (2010) 1325–1333.
[39] W.A. Mitch, D.L. Sedlak, Formation of N-nitrosodimethylamine (NDMA) from dimethylamine during chlorination, Environ. Sci. Technol. 36 (2002) 588–595.
[40] F.X. Tian, B. Xu, T.Y. Zhang, N.Y. Gao, Degradation of phenylurea herbicides by chlorine dioxide and formation of disinfection by-products during subsequent chlor(am)ination, Chem. Eng. J. 258 (2014) 210–217.
[41] F.X. Tian, X.J. Hu, B. Xu, T.Y. Zhang, Y.Q. Gao, Phototransformation of iodate by *UV* irradiation: kinetics and iodinated trihalomethane formation during subsequent chlor(am)ination, J. Hazard. Mater. 326 (2017) 138–144.
[42] D. Munch, D. Hautman, US EPA Method 551.1 Determination of Chlorination Disinfection Byproducts, Chlorinated Solvents, and Halogenated Pesticides/Herbicides in Drinking Water by Liquid-Liquid Extraction and Gas Chromatography with Electroncapture Detection, US EPA, Cincinnati, Ohio, 1995.
[43] J. De Laat, H. Gallard, Catalytic decomposition of hydrogen peroxide by Fe (III) in homogeneous aqueous solution: mechanism and kinetic modeling, Environ. Sci. Technol. 33 (1999) 2726–2732.
[44] A.P.H. Association, Standard Methods for the Examination of Water and Wastewater, American Public Health Association, Washington, DC, 1998 (1268).
[45] W.L. Wang, Q.Y. Wu, N. Huang, T. Wang, H.Y. Hu, Synergistic effect between *UV* and chlorine (*UV*/chlorine) on the degradation of carbamazepine: influence factors and radical species, Water Res. 98 (2016) 190–198.
[46] D. Miklos, W.L. Wang, K. Linden, J. Drewes, U. Hübner, Comparison of *UV*-AOPs (*UV*/H_2O_2, *UV*/*PDS* and *UV*/Chlorine) for TOrC removal from municipal wastewater effluent and optical surrogate model evaluation, Chem. Eng. J. 362 (2019) 537–547.
[47] P. Sun, T. Meng, Z. Wang, R. Zhang, H. Yao, Y. Yang, L. Zhao, Degradation of organic micropollutants in *UV*/NH_2Cl advanced oxidation process, Environ. Sci. Technol. 53 (2019) 9024–9033.
[48] F.M. Wendel, C. Lütke Eversloh, E.J. Machek, S.E. Duirk, M.J. Plewa, S.D. Richardson, T.A. Ternes, Transformation of iopamidol during chlorination, Environ. Sci. Technol. 48 (2014) 12689–12697.
[49] Z. Wu, C. Chen, B.Z. Zhu, C.H. Huang, T. An, F. Meng, J. Fang, Reactive nitrogen species are also involved in the transformation of micropollutants by the *UV*/monochloramine process, Environ. Sci. Technol. 53 (2019) 11142–11152.
[50] H.H. Alshamsi, H.K. Al, Shdood, *UV*-ClO_2 assisted decolorization of methylene blue, J. Chem. Pharm. Res. 7 (2015) 36–44.
[51] H.A. Habeeb, H.A. Khayoon, COD and color mineralization of azure C dye using *UV*/ClO_2 technique, J. Educ. Pure Sci. 5 (2015) 46–67.
[52] H.H. Alshamsi, H.K. Al shdood, Color and COD removal of Azure C dye by UV-ClO2 photochemical oxidation, Int. J. Chem. Sci. 14 (2016) 1296-1306.
[53] F.J. Beltrán, M. González, F.J. Rivas, P. Alvarez, Aqueous *UV* radiation and *UV*/H_2O_2 oxidation of atrazine first degradation products: deethylatrazine and deisopropylatrazine, Environ. Toxicol. Chem. 15 (1996) 868–872.
[54] B. Xu, N.Y. Gao, X.F. Sun, S.J. Xia, M. Rui, M.O. Simonnot, C. Causserand, J.F. Zhao, Photochemical degradation of diethyl phthalate with *UV*/H_2O_2, J. Hazard. Mater. 139 (2007) 132–139.
[55] F.H. AlHamedi, M. Rauf, S.S. Ashraf, Degradation studies of Rhodamine B in the presence of *UV*/H_2O_2, Desalination 239 (2009) 159–166.
[56] F.X. Tian, S.X. Ma, B. Xu, X.J. Hu, H.B. Xing, J. Liu, J. Wang, Y.Y. Li, B. Wang, X. Jiang, Photochemical degradation of iodate by *UV*/H_2O_2 process: kinetics, parameters and enhanced formation of iodo-trihalomethanes during chloramination, Chemosphere 221 (2019) 292–300.
[57] F.X. Tian, B. Xu, Y.L. Lin, C.Y. Hu, T.Y. Zhang, S.J. Xia, W.H. Chu, N.Y. Gao, Chlor(am)ination of iopamidol: kinetics, pathways and disinfection by-products formation, Chemosphere 184 (2017) 489–497.
[58] Y. Feng, D.W. Smith, J.R. Bolton, Photolysis of aqueous free chlorine species (*HOCl* and OCl^-) with 254 nm ultraviolet light, J. Environ. Eng. Sci. 6 (2007) 277–284.
[59] J. Jeong, J. Jung, W.J. Cooper, W. Song, Degradation mechanisms and kinetic studies for the treatment of X-ray contrast media compounds by advanced oxidation/reduction processes, Water Res. 44 (2010) 4391–4398.
[60] H. Dong, Z. Qiang, J. Hu, J. Qu, Degradation of chloramphenicol by *UV*/chlorine treatment: kinetics, mechanism and enhanced formation of halonitromethanes, Water Res. 121 (2017) 178–185.
[61] X. Kong, J. Jiang, J. Ma, Y. Yang, W. Liu, Y. Liu, Degradation of atrazine by *UV*/chlorine: efficiency, influencing factors, and products, Water Res. 90 (2016) 15–23.
[62] J.E. Grebel, J.J. Pignatello, W.A. Mitch, Effect of halide ions and carbonates on organic contaminant degradation by hydroxyl radical-based advanced oxidation processes in saline waters, Environ. Sci. Technol. 44 (2010) 6822–6828.
[63] R. Zhang, T. Meng, C.H. Huang, W. Ben, H. Yao, R. Liu, P. Sun, PPCP degradation by chlorine-*UV* processes in ammoniacal water: new reaction insights, kinetic modeling, and DBP formation, Environ. Sci. Technol. 52 (2018) 7833–7841.
[64] Y. Wu, S. Zhu, W. Zhang, L. Bu, S. Zhou, Comparison of diatrizoate degradation by *UV*/chlorine and *UV*/chloramine processes: Kinetic mechanisms and iodinated disinfection byproducts formation, Chem. Eng. J. 375 (2019) 121972.
[65] J. Li, E.R. Blatchley, Iii, *UV* photodegradation of inorganic chloramines, Environ. Sci. Technol. 43 (2009) 60–65.

[66] W. Liu, Z. Zhang, X. Yang, Y. Xu, Y. Liang, Effects of *UV* irradiation and *UV*/chlorine co-exposure on natural organic matter in water, Sci. Total Environ. 414 (2012) 576–584.
[67] D. Wang, J.R. Bolton, R. Hofmann, Medium pressure *UV* combined with chlorine advanced oxidation for trichloroethylene destruction in a model water, Water Res. 46 (2012) 4677–4686.
[68] Z. Hua, K. Guo, X. Kong, S. Lin, Z. Wu, L. Wang, H. Huang, J. Fang, PPCP degradation and DBP formation in the solar/free chlorine system: Effects of pH and dissolved oxygen, Water Res. 150 (2019) 77–85.
[69] M. Deinzer, F. Schaumburg, E. Klein, Environmental health sciences center task force review on halogenated organics in drinking water, Environ. Health Perspect. 24 (1978) 209–239.
[70] P.J. Vikesland, K. Ozekin, R.L. Valentine, Monochloramine decay in model and distribution system waters, Water Res. 35 (2001) 1766–1776.
[71] J.J. Lin, D.W. Hwang, Y.T. Lee, X. Yang, Photodissociation dynamics of *OClO* at 157 nm, J. Chem. Phys. 108 (1998) 10061–10069.
[72] H.F. Davis, Y.T. Lee, Photodissociation dynamics of *ClO* radicals at 248 nm, J. Phys. Chem. 100 (1996) 30–34.
[73] V. Vaida, J.D. Simon, The photoreactivity of chlorine dioxide, Science 268 (1995) 1443–1448.
[74] V. Vaida, S. Solomon, E.C. Richard, E. Rühl, A. Jefferson, Photoisomerization of *OClO*: a possible mechanism for polar ozone depletion, Nature 342 (1989) 405–408.
[75] J.L. Wang, L.J. Xu, Advanced oxidation processes for wastewater treatment: formation of hydroxyl radical and application, Crit. Rev. Environ. Sci. Technol. 42 (2012) 251–325.
[76] J. Wang, M. Song, B. Chen, L. Wang, R. Zhu, Effects of pH and H_2O_2 on ammonia, nitrite, and nitrate transformations during UV_{254} nm irradiation: implications to nitrogen removal and analysis, Chemosphere 184 (2017) 1003–1011.
[77] J. Mack, J.R. Bolton, Photochemistry of nitrite and nitrate in aqueous solution: a review, J. Photochem. Photobiol., A 128 (1999) 1–13.
[78] S.P. Mezyk, A.J. Elliot, Pulse radiolysis of lodate in aqueous solution, J. Chem. Soc., Faraday Trans. 90 (1994) 831–836.
[79] G.V. Buxton, C.L. Greenstock, W.P. Helman, A.B. Ross, Critical review of rate constants for reactions of hydrated electrons, hydrogen atoms and hydroxyl radicals ($\cdot OH/\cdot O^-$) in aqueous solution, Journal of Physical and Chemical Reference Data, J. Phys. Chem. Ref. Data. 17 (1988) 513–886.
[80] N. Daneshvar, A. Aleboyeh, A. Khataee, The evaluation of electrical energy per order (EEO) for photooxidative decolorization of four textile dye solutions by the kinetic model, Chemosphere 59 (2005) 761–767.
[81] J.R. Bolton, K.G. Bircher, W. Tumas, C.A. Tolman, Figures-of-merit for the technical development and application of advanced oxidation technologies for both electric- and solar-driven systems (IUPAC Technical Report), Pure Appl. Chem. 73 (2001) 627–637.
[82] Y. Xiao, L. Zhang, J. Yue, R.D. Webster, T.T. Lim, Kinetic modeling and energy efficiency of UV/H_2O_2 treatment of iodinated trihalomethanes, Water Res. 75 (2015) 259–269.
[83] K. Guo, Z. Wu, S. Yan, B. Yao, W. Song, Z. Hua, X. Zhang, X. Kong, X. Li, J. Fang, Comparison of the *UV*/chlorine and UV/H_2O_2 processes in the degradation of PPCPs in simulated drinking water and wastewater: kinetics, radical mechanism and energy requirements, Water Res. 147 (2018) 184–194.
[84] C.H. Wu, C.H. Lai, W.Y. Chung, Electrical energy per order and photodegradation efficiency of advanced oxidation processes, Appl. Mech. Mater. Trans Tech Publ. Ltd. 291 (2013) 764–767.
[85] H. Chen, T. Lin, W. Chen, H. Xu, H. Tao, Different removal efficiency of disinfection-byproduct precursors between dichloroacetonitrile (DCAN) and dichloroacetamide (DCAcAm) by up-flow biological activated carbon (UBAC) process, Environ. Sci. Pollut. Res. 26 (2019) 25874–25882.
[86] K.E. Furst, B.M. Pecson, B.D. Webber, W.A. Mitch, Tradeoffs between pathogen inactivation and disinfection byproduct formation during sequential chlorine and chloramine disinfection for wastewater reuse, Water Res. 143 (2018) 579–588.
[87] X. Duan, X. He, D. Wang, S.P. Mezyk, S.C. Otto, R. Marfil-Vega, M.A. Mills, D.D. Dionysiou, Decomposition of iodinated pharmaceuticals by *UV*-254 nm-assisted advanced oxidation processes, J. Hazard. Mater. 323 (2017) 489–499.
[88] T. Ye, B. Xu, Y.L. Lin, C.Y. Hu, L. Lin, T.Y. Zhang, N.Y. Gao, Formation of iodinated disinfection by-products during oxidation of iodide-containing waters with chlorine dioxide, Water Res. 47 (2013) 3006–3014.
[89] F. El-Athman, M. Jekel, A. Putschew, Reaction kinetics of corrinoid-mediated deiodination of iodinated X-ray contrast media and other iodinated organic compounds, Chemosphere 234 (2019) 971–977.
[90] C. Cortés, R. Marcos, Genotoxicity of disinfection byproducts and disinfected waters: a review of recent literature, Mutat. Res., Genet. Toxicol. Environ. Mutagen. 831 (2018) 1–12.
[91] I.A. Ike, Y. Lee, J. Hur, Impacts of advanced oxidation processes on disinfection byproducts from dissolved organic matter upon post-chlor(am)ination: a critical review, Chem. Eng. J. 121929 (2019).
[92] F. Yang, Z. Yang, H. Li, F. Jia, Y. Yang, Occurrence and factors affecting the formation of trihalomethanes, haloacetonitriles and halonitromethanes in outdoor swimming pools treated with trichloroisocyanuric acid, Environ. Sci. Water Res. Technol. 4 (2018) 218–225.
[93] S. Navalon, M. Alvaro, H. Garcia, Chlorine dioxide reaction with selected amino acids in water, J. Hazard. Mater. 164 (2009) 1089–1097.
[94] Z.C. Gao, Y.L. Lin, B. Xu, Y. Xia, C.Y. Hu, T.C. Cao, X.Y. Zou, N.Y. Gao, Evaluating iopamidol degradation performance and potential dual-wavelength synergy by *UV*-LED irradiation and *UV*-LED/chlorine treatment, Chem. Eng. J. 360 (2019) 806–816.